Hindawi
Journal of Applied Mathematics
Volume 2022, Article ID 1095441, 21 pages
https://doi.org/10.1155/2022/1095441

Research Article

Bifurcation Analysis of a 5D Nutrient, Plankton, *Limnothrissa miodon* Model with *Hydrocynus vittatus* Predation

Farikayi K. Mutasa,[1] **Brian Jones**,[2] **Itai H. Tendaupenyu**,[3] **Tamuka Nhiwatiwa**,[4] **and Mzime R. Ndebele-Murisa**[5]

[1]*Department of Applied Mathematics, National University of Science and Technology, P.O. Box AC939, Ascot, Bulawayo, Zimbabwe*
[2]*Department of Statistics and Operations Research, National University of Science and Technology, P.O. Box AC939, Ascot, Bulawayo, Zimbabwe*
[3]*The Zimbabwe Parks and Wildlife Management Authority, Cnr Sandringham & Borrowdale Rd, Botanical Gardens, PO BOX CY140, Causeway Harare, Zimbabwe*
[4]*Department of Biological Sciences, University of Zimbabwe, P.O. MP167 Mt. Pleasant, Harare, Zimbabwe*
[5]*School of Wildlife and Ecology, Chinhoyi University of Technology, Chinhoyi, Zimbabwe*

Correspondence should be addressed to Farikayi K. Mutasa; farikayi.mutasa@nust.ac.zw

Received 4 April 2022; Revised 29 June 2022; Accepted 1 July 2022; Published 20 July 2022

Academic Editor: Wei-Chiang Hong

In this paper, we construct and analyze a theoretical, deterministic 5D mathematical model of *Limnothrissa miodon* with nutrients, phytoplankton, zooplankton, and *Hydrocynus vittatus* predation. Local stability analysis results agree with the numerical simulations in that the coexistence equilibrium is locally stable provided that certain conditions are satisfied. The coexistence equilibrium is globally stable if certain conditions are met. Existence, stability, and direction of Hopf bifurcations are derived for some parameters. Bifurcation analysis shows that the model undergoes Hopf bifurcation at the coexistence point for the zooplankton growth rate with periodic doubling leading to chaos.

1. Introduction

Hydrocynus vittatus (Castelnau, 1861), also referred to as tigerfish, is the major predator of *Limnothrissa miodon* (Boulenger, 1906), also referred to as kapenta in Lake Kariba [1]. It is therefore important to investigate mathematically the role that tigerfish plays in the dynamics of *Limnothrissa miodon*. This paper begins by formulating and analyzing a deterministic *Limnothrissa miodon* model. The model has 5 classes, and these are as follows: concentration of nutrients, population density of phytoplankton, zooplankton population density, density of the *Limnothrissa miodon* population, and population density of tigerfish. The densities in each class are functions of time and are denoted by $N(t)$, $P(t)$, $Z(t)$, $L(t)$, and $R(t)$, respectively. The model is analyzed to determine the effect of predation on the population density of *Limnothrissa miodon* using qualitative techniques. Numerical simulations are done to illustrate the dynamics of the *Limnothrissa miodon* model.

Mathematical modeling of the *Limnothrissa miodon* model with tigerfish predation will give us an insight into the dynamics of the kapenta fishery in Lake Kariba. A deterministic model that involves nutrients, phytoplankton, zooplankton, *Limnothrissa miodon*, and tigerfish has not been formulated and analyzed. In this paper, we formulate and analyze a deterministic, continuous, dynamical system which consists of ordinary differential equations that describe the dynamics of *Limnothrissa miodon* in the presence of nutrients, phytoplankton, and zooplankton and with tigerfish predation. The *Limnothrissa miodon* model will help in our understanding of the dynamics of the aquatic ecosystem in the kapenta fishery in Lake Kariba.

The major predator in Lake Kariba is tigerfish [2, 3], and after the introduction of *Limnothrissa miodon* into Lake

Kariba, they became a major prey item for tigerfish. Since kapenta inhabit deeper pelagic waters, tigerfish are now also found in that habitat close to the surface. According to Bell-Cross [4], the tigerfish is an efficient and extremely active predator which preys on fish of up to 40% its length. A number of studies have been done to assess the diet of *Hydrocynus vittatus* [5–8]. Results from the study by Mhlanga [7] showed that *Limnothrissa miodon* is the dominant food item in the diet of the piscivorous *Hydrocynus vittatus*. Stable isotope analysis by Marufu et al. [8] showed that *Limnothrissa miodon* is still the dominant food item consumed by tigerfish. Mhlanga [9] obtained a natural, fishing, total mortality, and exploitation rate of 0.66, 0.335, 0.995, and 0.337, respectively, of tigerfish from the Bumi Basin of Lake Kariba and the Ume River. Balon [10] obtained an instantaneous mortality coefficient for the inshore tigerfish of 0.52, which was similar to the one obtained by Langerman [11] of 0.58. Marshall [12] obtained a correlation of $r = 0.89$ between the abundance of *Limnothrissa miodon* and *Hydrocynus vittatus*. Takano and Subramaniam [13] concluded in their study that tigerfish predation and increased fishing pressure are the major factors contributing to the natural mortality of *Limnothrissa miodon*.

Pal and Chatterjee [14] showed the existence of Hopf bifurcations for the phytoplankton growth rate, phytoplankton carrying capacity, time delay, and fish mortality rate, in a plankton-fish model. According to Raw et al. [15], a stable interior point, period-one limit cycles, multiple-period cycles, and chaotic attractors were observed for the zooplankton growth rate bifurcation parameter in a plankton-fish model. They suggested that chaos in plankton-fish dynamics is a result of an excess of predation rate. A hopf bifurcation was observed for the phytoplankton growth rate and harvesting effort [15]. Panja and Jana [16] investigated a plankton-fish model and found that zooplankton consumption rate, fish harvesting rate, and half saturation significantly alter the model stability through a Hopf bifurcation as the parameters are varied.

Dynamical systems have not been used to understand how tigerfish predation describes and influences the dynamics of kapenta fish populations in Lake Kariba. By formulating a mathematical model and analyzing it, we will be able to qualitatively explain the impact of predation on the levels of kapenta fish. The qualitative behavior of the solutions of the dynamical system is investigated for a set of parameters through bifurcation analysis.

The remainder of this paper presents the materials and methods which describe the study area, data collection in Section 2; model formulation, positivity, and existence of solutions in Section 3; equilibrium states and their stability in Section 4; and bifurcation analysis in Section 5. Numerical simulations are presented in Section 6, and concluding remarks in Section 7.

2. Materials and Methods

2.1. Study Area. Lake Kariba (277 km long; about 5364 km^2 in surface area; 160 km^3 capacity; 29 m mean depth; and 120 m maximum depth) is located in a tropical area with seasonal rainfall on the Zambezi River between latitudes 1628′ to 1804′S and longitudes 2642′ to 2903′E [17] and was formed by damming the Zambezi River at the Kariba gorge in 1958 and was filled in 1963 [18]. Lake Kariba has an average width of 19.4 km, although the widest portion is 40 km, and is 486 m above sea level, and the shoreline is approximately 2164 km [19]. The lake is almost equally shared by the two riparian countries, Zambia and Zimbabwe, and its catchment area covers 663817 km^2 extending over parts of Angola, Zambia, Namibia, Botswana, and Zimbabwe [20]. The offshore single-species pelagic kapenta fishery is highly mechanized and performed by light attraction and lift nets from pontoon rigs and is licence-controlled [21].

2.2. Data Collection. The data used in this study was obtained from the Lake Kariba Fisheries Research Institute (LKFRI) and the University of Zimbabwe Lake Kariba Research Station (UZLKRS). The Lake Kariba Fisheries Research Institute collects data on catch, effort in the experimental gillnet, inshore artisanal, and offshore kapenta fisheries. The catch data is measured in metric tonnes (wet weight), and fishing effort is the number of nights fished. The CPUE is the kapenta catch that is landed by a boat after a night of fishing and is measured in tonnes/boat/night. It is an important parameter in fisheries management as it is an indicator of fish abundance and economic performance of the fishery [22]. The University of Zimbabwe Lake Kariba Research Institute collects data on water quality of the lake. Figure 1 shows the monthly average time series of kapenta catch and tigerfish bycatch in tonnes in the Lake Kariba kapenta fishery from 1974 to 2018.

The predator-prey relationship between the tigerfish and kapenta is shown in Figure 1. From Figure 1, it is apparent that the tigerfish bycatch and kapenta catch show cyclical behavior and that the tigerfish bycatch generally tracks the peaks in the kapenta catch.

3. Model Formulation

The model has 5 classes: N denoting the concentration of nutrients, P is the population density of phytoplankton, Z is the zooplankton population density, L is the density of the *Limnothrissa miodon* population, and R is the density of the *Hydrocynus vittatus* population. The densities in each class are functions of time and are denoted by $N(t)$, $P(t)$, $Z(t)L(t)$, and $R(t)$, respectively. The *Limnothrissa miodon* model [23] is developed to include predation by *Hydrocynus vittatus*. It is assumed that nutrients enter the water body at the rate a, where $a > 0$ is a constant and the nutrients are depleted naturally at a constant rate μ_0. The nutrients are depleted by phytoplankton at a rate of $\sigma_1 NP$. The growth rate of phytoplankton is $\gamma_1 NP$. It is assumed that the depletion rate of phytoplankton caused by mortality is proportional to P. Phytoplankton is depleted by zooplankton at a rate $\sigma_2 PZ$. The depletion of phytoplankton per unit time by zooplankton is given by $\sigma_2 PZ$ and is the modified Holling's type I response [24], which refers to the change in density of the phytoplankton per unit time per zooplankton as the phytoplankton population density changes. The growth rate of zooplankton is $\gamma_2 PZ$. It is assumed that the depletion rate of zooplankton caused by mortality is proportional to Z.

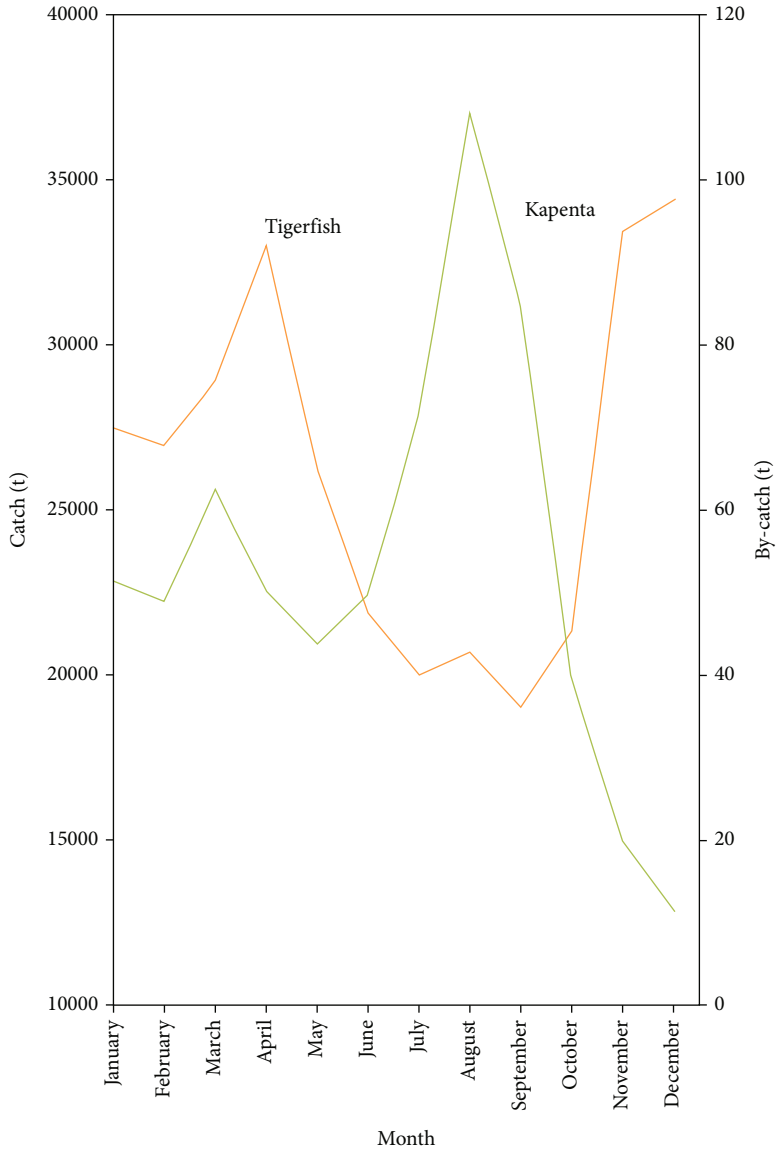

Figure 1: Time series plot of kapenta and tigerfish catch.

The functional response of zooplankton to the *Limnothrissa miodon* given by $\sigma_3 ZL$ is of the modified Holling's type I response, which refers to the change in density of the zooplankton per unit time per *Limnothrissa miodon* as the zooplankton population density changes. The growth rate of *Limnothrissa miodon* is $\gamma_3 ZL$. It is assumed that the depletion rate of *Limnothrissa miodon* caused by mortality is proportional to L and its rate of depletion caused by crowding is proportional to L^2. Kapenta are harvested at a rate qEL, where q is the catchability coefficient and E is the effort measured as boat nights. Tigerfish search and feed on kapenta; therefore, we use Holling's type II functional response. The feeding rate saturates at the maximum feeding rate σ_4. The feeding rate is half maximal at $L = d$. The response $f(L) = (\sigma_4 L/d + L)$ [25] models the fact that the consumption of kapenta is limited by satiation of tigerfish, handling time (killing and eating) and time spent hunting kapenta. The growth rate of *Limnothrissa miodon* is $\gamma_4 LR/d + L$. The tigerfish are harvested at a rate $\kappa\eta R$, where κ is the catchability coefficient and η is the effort. The nonlinear dynamical system is

$$\begin{cases} \dfrac{dN}{dt} = a - \mu_0 N - \sigma_1 NP, \\ \dfrac{dP}{dt} = \gamma_1 NP - \mu_1 P - \sigma_2 PZ, \\ \dfrac{dZ}{dt} = \gamma_2 PZ - \mu_2 Z - \sigma_3 ZL, \\ \dfrac{dL}{dt} = \gamma_3 ZL - \mu_3 L - \sigma_{30} L^2 - qEL - \dfrac{\sigma_4 LR}{d + L}, \\ \dfrac{dR}{dt} = \dfrac{\gamma_4 LR}{d + L} - \kappa\eta R - \mu_4 R, \end{cases} \tag{1}$$

with initial condition

$$\begin{cases} N(0) = \psi_1(0), P(0) = \psi_2(0), \\ Z(0) = \psi_3(0), L(0) = \psi_4(0), \\ R(0) = \psi_5(0), \psi_i(0) > 0, i = 1, 2, 3, 4, 5. \end{cases} \tag{2}$$

and define

$$\Omega = \left\{(N, P, Z, L, R) \in \mathbb{R}^5 | N \geq 0, P \geq 0, Z \geq 0, L \geq 0, R \geq 0\right\}, \tag{3}$$

to be the mathematically feasible region. The coefficient σ_{30} is a positive constant for the crowding of the *Limnothrissa miodon* population. σ_1, σ_2, σ_3, σ_4 are positive constants of proportionality. The μ_i's for $i = 0, 1, 2, 3, 4$ are the depletion rate coefficients.

3.1. Positivity of Solutions. Model system (1) describes the dynamics of an ecosystem and it is necessary to prove that the concentrations of nutrients, and the densities of phytoplankton, zooplankton, and kapenta are positive for all time. For positive initial data for the ecosystem model (1), we prove that the solutions will remain positive $\forall t \geq 0$.

Theorem 1. *Let the initial data be $N(t) \geq 0, P(t) \geq 0, Z(t) \geq 0, L(t) \geq 0, R(t) \geq 0$. Then, solutions of $N(t)$, $P(t)$, $Z(t)$, $L(t)$, $R(t)$ of system (1) are positive $\forall t \geq 0$.*

Proof. Considering the variable $N(t)$ in $[0, T]$, from the first equation of model (1), it follows that

$$\dot{N}(t) \geq -\mu_0 N(t) - \sigma_1 N(t) P(t), \forall t \in [0, T]. \tag{4}$$

Hence, we obtain

$$N(t) \geq N(0) \exp \int_0^t (-\mu_0 - \sigma_1 P(s)) ds \geq 0, \forall t \in [0, T]. \tag{5}$$

From the second equation of model (1), it follows that

$$\dot{P}(t) \geq -\mu_1 P(t) - \sigma_2 P(t) Z(t), \forall t \in [0, T]. \tag{6}$$

Direct integration of (6) results in

$$P(t) \geq P(0) \exp \int_0^t (-\mu_1 - \sigma_2 Z(s)) ds \geq 0, \forall t \in [0, T]. \tag{7}$$

From the third equation of model (1), it follows that

$$\dot{Z}(t) \geq -\mu_2 Z(t) - \sigma_3 Z(t) L(t), \forall t \in [0, T]. \tag{8}$$

Direct integration of (8) results in

$$Z(t) \geq Z(0) \exp \int_0^t (-\mu_2 - \sigma_3 L(s)) ds \geq 0, \forall t \in [0, T]. \tag{9}$$

Considering the variable $L(t)$ in $[0, T]$, from the fourth equation of model (1), it follows that

$$\dot{L}(t) \geq -\left(\mu_3 + qE + \sigma_{30} L(t) + \frac{\sigma_4 R(t)}{d + L(t)}\right) L(t), \forall t \in [0, T]. \tag{10}$$

Direct integration of (10) results in

$$L(t) \geq L(0) \exp \left[-\int_0^t \left(\mu_3 + qE + \sigma_{30} L(s) + \frac{\sigma_4 R(s)}{d + L(s)}\right) ds\right] \geq 0, \forall t \in [0, T]. \tag{11}$$

From the fifth equation of model (1), it follows that

$$\dot{R}(t) \geq -(\mu_4 + \kappa\eta) R(t), \forall t \in [0, T]. \tag{12}$$

Direct integration of (12) results in

$$R(t) \geq R(0) \exp\left(-(\mu_4 + \kappa\eta) t\right) \geq 0, \forall t \in [0, T]. \tag{13}$$

Therefore, the solutions of system (1) with initial condition (2) remains positive $\forall t \geq 0$. □

3.2. Existence of Solutions

Theorem 2. *A solution of model system (1) is feasible.*

Proof. It is necessary to show that system (1) is dissipative; that is, all feasible solutions are uniformly bounded in $\Omega \subset \mathbb{R}^5$. Let $\{(N(t), P(t), Z(t), L(t), R(t)) \in \mathbb{R}^5\}$ be any solution of system (1) with nonnegative initial conditions.

Let $A(t) = N(t) + P(t) + Z(t) + L(t) + R(t)$, then

$$\begin{aligned} \frac{dA}{dt} &= a - \mu_0 N - \sigma_1 NP + \gamma_1 NP - \mu_1 P - \sigma_2 PZ + \gamma_2 PZ - \mu_2 Z \\ &\quad - \sigma_3 ZL + \gamma_3 ZL - \mu_3 L - \sigma_{30} L^2 - qEL - \frac{\sigma_4 LR}{d + L} + \frac{\gamma_4 LR}{d + L} \\ &\quad - \kappa\eta R - \mu_4 R, = a - \mu_0 N - \mu_1 P - \mu_2 Z - (\mu_3 + qE) L \\ &\quad - \sigma_{30} L^2 - \kappa\eta R - \mu_4 R + (\gamma_1 - \sigma_1) NP + (\gamma_2 - \sigma_2) PZ \\ &\quad + (\gamma_3 - \sigma_3) ZL + (\gamma_4 - \sigma_4) \frac{LR}{d + L}, \leq a - \mu_0 N - \mu_1 P \\ &\quad - \mu_2 Z - (\mu_3 + qE) L - (\kappa\eta + \mu_4) R, \leq a - uA(t), \end{aligned} \tag{14}$$

where $u = \min\{(\mu_0, \mu_1, \mu_2, \mu_3 + qE, \kappa\eta + \mu_4)\}$. Thus,

$$\frac{dA(t)}{dt} + uA(t) \leq a. \tag{15}$$

The solution to Equation (15) is

$$0 < A(N, P, Z, L, R) \leq \frac{a}{u}\left(1 - e^{-ut}\right) + A(N_0, P_0, Z_0, L_0, R_0) e^{-ut}, \tag{16}$$

as $t \longrightarrow \infty$, (16) becomes

$$0 < A(N, P, Z, L, R) \leq \frac{a}{u}. \tag{17}$$

Therefore, all solutions of the system (1) enter the feasible region,

$$\Omega = \left\{ (N(t), P(t), Z(t), L(t), R(t)) \in \mathbb{R}_+^5 : A \leq \frac{a}{u} + \varsigma, \forall \varsigma > 0 \right\}. \tag{18}$$

This completes the proof of the theorem. □

4. Equilibria and Stability Analysis

Model (1) has 6 equilibria:

(a) The trivial equilibrium is

$$E_0 = (0, 0, 0, 0, 0). \tag{19}$$

(b) The phytoplankton free equilibrium is

$$E_1 = (N_1^*, 0, 0, 0, 0) = \left(\frac{a}{\mu_0}, 0, 0, 0, 0 \right). \tag{20}$$

(c) The zooplankton free equilibrium is

$$E_2 = (N_2^*, P_2^*, 0, 0, 0), = \left(\frac{\mu_1}{\gamma_1}, \frac{a\gamma_1 - \mu_1\mu_0}{\sigma_1\mu_1}, 0, 0, 0 \right). \tag{21}$$

E_2 is obtained when phytoplankton is taking part in the ecosystem, and zooplankton and *Limnothrissa miodon* are not taking part in the ecosystem. The phytoplankton population is not enough to support the zooplankton population. E_2 exists provided that

$$a\gamma_1 > \mu_1\mu_0. \tag{22}$$

Rearranging the inequality (22), we obtain $(a/\mu_0) > (\mu_1/\gamma_1)$, and this means that $N_1^* > N_2^*$. The nutrients will reach the value a/μ_0 at equilibrium in the absence of phytoplankton, which is reduced to the steady state value of μ_1/γ_1 in the presence of phytoplankton.

(d) The *Limnothrissa miodon* free equilibrium is

$$\begin{gathered} E_3 = (N_3^*, P_3^*, Z_3^*, 0, 0), \\ E_3 = \left(\frac{a}{\mu_0 + \sigma_1 P_3^*}, \frac{\mu_2}{\gamma_2}, \frac{\gamma_1 N_3^* - \mu_1}{\sigma_2}, 0, 0 \right). \end{gathered} \tag{23}$$

The zooplankton population is insufficient to support the population of *Limnothrissa miodon*. When the *Limnothrissa miodon* population is not present in the ecosystem and both phytoplankton and zooplankton are present, E_3 is attained. E_3 exists if $N_3^* > \mu_1/\mu_1$, i.e. $N_3^* > N_2^*$. In order to support the zooplankton population, more nutrients are needed in the ecosystem. From (23),

$$E_3 = \left(\frac{a\gamma_2}{\gamma_2\mu_0 + \mu_2\sigma_1}, \frac{\mu_2}{\gamma_2}, \frac{a\gamma_1\gamma_2 - \mu_1(\gamma_2\mu_0 + \mu_2\sigma_1)}{\sigma_2(\gamma_2\mu_0 + \mu_2\sigma_1)}, 0, 0 \right). \tag{24}$$

E_3 exists on condition that

$$\frac{a\gamma_1 - \mu_0\mu_1}{\sigma_1\mu_1} > \frac{\mu_2}{\gamma_2}. \tag{25}$$

Inequality (25) can be rearranged to give $P_2^* > P_3^*$, meaning that the phytoplankton equilibrium is reduced in the presence of zooplankton.

(e) The tigerfish free equilibrium $E_4 = (N_4^*, P_4^*, Z_4^*, L_4^*, 0)$ is obtained by solving the equations:

$$a - \mu_0 N - \sigma_1 NP = 0, \tag{26}$$

$$\phi_1\sigma_1 N - \mu_1 - \sigma_2 Z = 0, \tag{27}$$

$$\phi_2\sigma_2 P - \mu_2 - \sigma_3 L = 0, \tag{28}$$

$$\phi_3\sigma_3 Z - \mu_3 - eq - \sigma_{30} L = 0. \tag{29}$$

Solving for N, P, Z, and L in (26), (27), (28), and (29) gives

$$\begin{aligned} \sigma_1\sigma_2\sigma_3\sigma_{30}(L_4^*)^2 &+ (\sigma_1\sigma_2\sigma_3(\mu_3 + eq) + \sigma_1\sigma_2\mu_2\sigma_{30} \\ &+ \mu_0\sigma_2\gamma_2\sigma_{30} + \mu_1\sigma_1\sigma_3\gamma_3)L_4^* + \mu_0\mu_1\gamma_2\gamma_3 \\ &+ \mu_1\sigma_1\mu_2\gamma_3 + \mu_0\sigma_2\gamma_2(\mu_3 + eq) \\ &+ \sigma_1\sigma_2\mu_2(\mu_3 + eq) - a\gamma_1\gamma_2\gamma_3 = 0. \end{aligned} \tag{30}$$

Equation (31) will have a unique positive root if the expression (32) is positive,

$$L_4^* = \frac{\sqrt{A_1^2 - 4\sigma_1\sigma_2\sigma_3\sigma_{30}A_2} - A_1}{2\sigma_1\sigma_2\sigma_3\sigma_{30}} > 0, \tag{31}$$

where

$$\begin{gathered} A_1 = \sigma_1\sigma_2\sigma_3(\mu_3 + eq) + \sigma_1\sigma_2\mu_2\sigma_{30} + \mu_0\sigma_2\gamma_2\sigma_{30} + \mu_1\sigma_1\sigma_3\gamma_3, \\ \begin{aligned} A_2 = \mu_0\mu_1\gamma_2\gamma_3 &+ \mu_1\sigma_1\mu_2\gamma_3 + \mu_0\sigma_2\gamma_2(\mu_3 + eq) \\ &+ \sigma_1\sigma_2\mu_2(\mu_3 + eq) - a\gamma_1\gamma_2\gamma_3. \end{aligned} \end{gathered} \tag{32}$$

(31) can be written as

$$A_1^2 - 4\sigma_1\sigma_2\sigma_3\sigma_{30}A_2 > A_1^2,$$

$$\sigma_1\sigma_2\sigma_3\sigma_{30}A_2 < 0,$$
$$(\sigma_1\sigma_2\sigma_3\sigma_{30})(\mu_0\mu_1\gamma_2\gamma_3 + \mu_1\sigma_1\mu_2\gamma_3 + \mu_0\sigma_2\gamma_2(\mu_3 + eq) + \sigma_1\sigma_2\mu_2(\mu_3 + eq) - a\gamma_1\gamma_2\gamma_3) < 0,$$
$$\sigma_2(\mu_3 + eq)(\mu_0\gamma_2 + \sigma_1\mu_2) < \gamma_3(a\gamma_1\gamma_2 - (\mu_0\mu_1\gamma_2 + \mu_1\mu_2\sigma_1)),$$
$$\frac{\mu_3 + eq}{\gamma_3} < \frac{a\gamma_1\gamma_2 - (\mu_0\mu_1\gamma_2 + \mu_1\mu_2\sigma_1)}{\sigma_2(\mu_0\gamma_2 + \sigma_1\mu_2)},$$
$$\frac{\mu_3 + eq}{\gamma_3} < Z_3^*. \tag{33}$$

Therefore, L_4^* exists whenever

$$Z_3^* > \frac{\mu_3 + eq}{\gamma_3}. \tag{34}$$

The tigerfish free equilibrium is

$$N_4^* = \frac{(\mu_3 + eq)\sigma_1\sigma_2\sigma_3 - \mu_2\sigma_1\sigma_2\sigma_{30} - \mu_0\sigma_2\sigma_{30}\gamma_2 + \mu_1\sigma_1\sigma_3\gamma_3 + \sqrt{4A_3 + A_4^2}}{2\sigma_1\sigma_3\gamma_1\gamma_3},$$
$$P_4^* = \frac{-(\mu_3 + eq)\sigma_1\sigma_2\sigma_3 + \mu_2\sigma_1\sigma_2\sigma_{30} - \mu_0\sigma_2\sigma_{30}\gamma_2 - \mu_1\sigma_1\sigma_3\gamma_3 + \sqrt{4A_3 + A_4^2}}{2\sigma_1\sigma_2\sigma_{30}\gamma_2},$$
$$Z_4^* = \frac{(\mu_3 + eq)\sigma_1\sigma_2\sigma_3 - \mu_2\sigma_1\sigma_2\sigma_{30} - \mu_0\sigma_2\sigma_{30}\gamma_2 - \mu_1\sigma_1\sigma_3\gamma_3 + \sqrt{4A_3 + A_4^2}}{2\sigma_1\sigma_2\sigma_3\gamma_3},$$
$$L_4^* = \frac{-(\mu_3 + eq)\sigma_1\sigma_2\sigma_3 - \mu_2\sigma_1\sigma_2\sigma_{30} - \mu_0\sigma_2\sigma_{30}\gamma_2 - \mu_1\sigma_1\sigma_3\gamma_3 + \sqrt{4A_3 + A_4^2}}{2\sigma_1\sigma_2\sigma_3\sigma_{30}},$$
$$R_4^* = 0, \tag{35}$$

where

$$A_3 = a\sigma_1\sigma_2\sigma_3\sigma_{30}\gamma_1\gamma_2\gamma_3,$$
$$A_4 = (\mu_3 + eq)\sigma_1\sigma_2\sigma_3 - \sigma_2\sigma_{30}(\mu_2\sigma_1 + \mu_0\gamma_2) + \mu_1\sigma_1\sigma_3\gamma_3. \tag{36}$$

Remark 3. For some given set of parameter values, the model (1) has no equilibrium points.

Theorem 4. *The trivial equilibrium is always stable.*

From equation array (35), it follows that

$$N_4^* = \frac{(\mu_3 + eq)\sigma_1\sigma_2\sigma_3 - \mu_2\sigma_1\sigma_2\sigma_{30} - \mu_0\sigma_2\sigma_{30}\gamma_2 + \mu_1\sigma_1\sigma_3\gamma_3 + \sqrt{4A_3 + A_4^2}}{2\sigma_1\sigma_3\gamma_1\gamma_3},$$
$$P_4^* = \frac{\gamma_1\sigma_3\gamma_3N_4^* - (\mu_3 + eq)\sigma_2\sigma_3 + \mu_2\sigma_2\sigma_{30} - \mu_1\sigma_3\gamma_3}{\sigma_2\sigma_{30}\gamma_2},$$
$$Z_4^* = \frac{\sigma_{30}\gamma_2P_4^* + (\mu_3 + eq)\sigma_3 - \mu_2\sigma_{30}}{\sigma_3\gamma_3},$$
$$L_4^* = \frac{\gamma_3Z_4^* - (\mu_3 + eq)}{\sigma_{30}},$$
$$R_4^* = 0. \tag{37}$$

(f) The positive interior equilibrium of system (1) is the one of biological interest. For some set of parameter values, model (1) has a unique positive interior equilibrium, $E_* = (N^*, P^*, Z^*, L^*, R^*)$ which is obtained by solving the equations:

$$a - \mu_0N - \sigma_1NP = 0, \tag{38}$$
$$\gamma_1N - \mu_1 - \sigma_2Z = 0, \tag{39}$$
$$\gamma_2P - \mu_2 - \sigma_3L = 0, \tag{40}$$
$$\gamma_3Z - \mu_3 - \sigma_{30}L - qE - \frac{\sigma_4R}{d + L} = 0, \tag{41}$$
$$\frac{\gamma_4L}{d + L} - \kappa\eta - \mu_4 = 0. \tag{42}$$

Solving for N, P, Z, L, and R in (38), (39), (40), (41), and (42) gives the positive interior equilibrium

Proof. The auxilliary equation of the jacobian matrix at E_0 is

$$(\lambda + \mu_0)(\lambda + \mu_1)(\lambda + \mu_2)(\kappa + \lambda + \mu_4)(eq + \lambda + \mu_3) = 0. \tag{44}$$

The eigenvalues of (44) are $\lambda_1 = -\mu_0$, $\lambda_2 = -\mu_1$, $\lambda_3 = -\mu_2$, $\lambda_4 = -\kappa - \mu_4$, and $\lambda_5 = -eq - \mu_3$. All the eigenvalues are negative; therefore, E_0 is stable. □

$$N^* = \frac{a\gamma_2(-\gamma_4 + \kappa\eta + \mu_4)}{(\gamma_2\mu_0 + \mu_2\sigma_1)(-\gamma_4 + \kappa\eta + \mu_4) - d\sigma_1\sigma_3(\kappa\eta + \mu_4)},$$
$$P^* = \frac{\mu_2 - d\sigma_3(\kappa\eta + \mu_4)/-\gamma_4 + \kappa\eta + \mu_4}{\gamma_2},$$
$$Z^* = \frac{(-\gamma_4 + \kappa\eta + \mu_4)(a\gamma_1\gamma_2 - \mu_1(\gamma_2\mu_0 + \mu_2\sigma_1)) + d\mu_1\,\sigma_1\sigma_3(\kappa\eta + \mu_4)}{\sigma_2((\gamma_2\mu_0 + \mu_2\sigma_1)(-\gamma_4 + \kappa\eta + \mu_4) - d\,\sigma_1\sigma_3(\kappa\eta + \mu_4))},$$
$$L^* = \frac{d(\kappa\eta + \mu_4)}{\gamma_4 - (\kappa\eta + \mu_4)},$$
$$R^* = \frac{\gamma_4 d\left(((\gamma_2\mu_0 + \mu_2\sigma_1)(-\gamma_4 + \kappa\eta + \mu_4) - d\sigma_1\sigma_3(\kappa\eta + \mu_4))((-\gamma_4 + \kappa\eta + \mu_4)(\gamma_3\mu_1 + \sigma_2(eq + \mu_3)) - d\sigma_2\,\sigma_{30}(\kappa\eta + \mu_4)) - a\gamma_1\gamma_2\gamma_3(-\gamma_4 + \kappa\eta + \mu_4)^2\right)}{\sigma_2\sigma_4\,(-\gamma_4 + \kappa\eta + \mu_4)^2((\gamma_2\mu_0 + \mu_2\sigma_1)(-\gamma_4 + \kappa\eta + \mu_4) - d\sigma_1\sigma_3(\kappa\eta + \mu_4))}. \tag{43}$$

Theorem 5. *The phytoplankton free equilibrium is locally asymptotically stable if $a\gamma_1 < \mu_0\mu_1$.*

Proof. The auxilliary equation of the jacobian matrix at E_1 is

$$(\lambda+\mu_0)\left(-\lambda+\frac{a\gamma_1-\mu_0\mu_1}{\mu_0}\right)(\lambda+\mu_2)(\lambda+eq+\mu_3)\cdot(\lambda+\kappa+\mu_4)=0. \tag{45}$$

The eigenvalues are $\lambda_1=-\mu_0$, $\lambda_2=(a\gamma_1-\mu_0\mu_1/\mu_0)$, $\lambda_3=-\mu_2$, $\lambda_4=-eq-\mu_3$, $\lambda_5=-\kappa-\mu_4$.E_1 is asymptotically stable if $(a/\mu_0)<(\mu_1/\gamma_1)$, meaning that $N_1^*<N_1^*$ for stability of E_1. □

Theorem 6. *The zooplankton free equilibrium is locally asymptotically stable if $\sqrt{a^2\gamma_1^2-4a\gamma_1\mu_1^2+4\mu_0\mu_1^3}>0$, $(\gamma_2(a\gamma_1-\mu_0\mu_1)/\mu_1\sigma_1)<(\mu_2/\gamma_2)$, and $a\gamma_1>\mu_0\mu_1$.*

Proof. The auxilliary equation of the Jacobian matrix at E_2 is

$$(-\kappa-\lambda-\mu_4)(-eq-\lambda-\mu_3)((\gamma_2(a\gamma_1-\mu_0\mu_1)/\mu_1\sigma_1)-\lambda-\mu_2)\cdot\left(a\gamma_1^2\lambda\mu_1\sigma_1+a\gamma_1^2\mu_1^2\sigma_1+\gamma_1\lambda^2\mu_1^2\sigma_1-\gamma_1\mu_0\mu_1^3\sigma_1\right)=0. \tag{46}$$

The eigenvalues are $\lambda_1=-eq-\mu_3$, $\lambda_2=-\kappa-\mu_4$, $\lambda_3=(\gamma_2(a\gamma_1-\mu_0\mu_1)/\mu_1\sigma_1)-\mu_2$, $\lambda_4=-\sqrt{a^2\gamma_1^2-4a\gamma_1\mu_1^2+4\mu_0\mu_1^3}-a\gamma_1/2\mu_1$ and $\lambda_5=\sqrt{a^2\gamma_1^2-4a\gamma_1\mu_1^2+4\mu_0\mu_1^3}-a\gamma_1/2\mu_1$. Hence, E_2 is locally asymptotically stable if $\sqrt{a^2\gamma_1^2-4a\gamma_1\mu_1^2+4\mu_0\mu_1^3}>0$, $(\gamma_2(a\gamma_1-\mu_0\mu_1)/\mu_1\sigma_1)<(\mu_2/\gamma_2)$, and $a\gamma_1>\mu_0\mu_1$. □

Theorem 7. *The Limnothrissa miodon free equilibrium is locally asymptotically stable if the conditions in (50) are satisfied.*

Proof. The auxilliary equation of the jacobian matrix at E_3 is

$$(-\kappa-\lambda-\mu_4)(-b_1b_2\gamma_1\lambda\sigma_1-b_2b_3\gamma_2\lambda\sigma_2-b_2b_3\gamma_2\mu_0\sigma_2-b_2^2b_3\gamma_2\sigma_1\sigma_2-b_2\lambda^2\sigma_1-\lambda^3-\lambda^2\mu_0)\cdot(b_3\gamma_3-eq-\lambda-\mu_3)=0, \tag{47}$$

where $b_1=(a\gamma_2/\gamma_2\mu_0+\mu_2\sigma_1)$, $b_2=\mu_2/\gamma_2$, and $b_3=(a\gamma_1\gamma_2-\mu_1(\gamma_2\mu_0+\mu_2\sigma_1)/\sigma_2(\gamma_2\mu_0+\mu_2\sigma_1))$. The characteristic Equation (47) can be written as follows:

$$\Delta(\lambda)=a_0\lambda^5+a_1\lambda^4+a_2\lambda^3+a_3\lambda^2+a_4\lambda+a_5=0, \tag{48}$$

where

$$a_0=1,$$

$$a_1=b_2\sigma_1+eq+\kappa+\mu_0+\mu_3+\mu_4-b_3\gamma_3,$$

$$a_2=b_2\sigma_1(b_1\gamma_1+eq+\kappa+\mu_3+\mu_4)+b_3(b_2\gamma_2\sigma_2-\gamma_3(b_2\sigma_1+\kappa+\mu_0+\mu_4))+(\kappa+\mu_4)(eq+\mu_3)+\mu_0(eq+\kappa+\mu_3+\mu_4),$$

$$a_3=\mu_0(b_2b_3\gamma_2\sigma_2+(\kappa+\mu_4)(-b_3\gamma_3+eq+\mu_3))+b_2(\sigma_1((\kappa+\mu_4)(-b_3\gamma_3+eq+\mu_3)+b_1\gamma_1(-b_3\gamma_3+eq+\kappa+\mu_3+\mu_4))+b_3\gamma_2\sigma_2(-b_3\gamma_3+b_2\sigma_1+eq+\kappa+\mu_3+\mu_4)),$$

$$a_4=-b_2(b_1\gamma_1\sigma_1(\kappa+\mu_4)(-b_3\gamma_3+eq+\mu_3)+b_3\gamma_2\sigma_2(b_2\sigma_1(eq+\kappa+\mu_3+\mu_4)-b_3\gamma_3(b_2\sigma_1+\kappa+\mu_0+\mu_4)+(\kappa+\mu_4)(eq+\mu_3)+\mu_0(eq+\kappa+\mu_3+\mu_4))),$$

$$a_5=b_2b_3\gamma_2\sigma_2(\kappa+\mu_4)(b_2\sigma_1+\mu_0)(-b_3\gamma_3+eq+\mu_3). \tag{49}$$

By the Routh-Hurwitz criterion, it follows that all eigenvalues of the characteristic Equation (48) have negative real parts if

$$a_0>0,\ a_1>0,\ a_1a_2-a_0a_3>0,\ a_3(a_1a_2-a_0a_3)-a_1^2a_4>0,$$

$$a_1a_3a_4a_2+a_0a_3a_5a_2-a_1^2a_4^2-a_0^2a_5^2-a_0a_3^2a_4+2a_0a_1a_4a_5-a_1a_5a_2^2>0,\ a_5>0. \tag{50}$$

□

Theorem 8. *The tigerfish free equilibrium is locally asymptotically stable if the conditions in (54) are satisfied.*

Proof. The auxilliary equation of the jacobian matrix at E_4 is

$$\begin{aligned}&\lambda^5+\lambda^4(-A_1-A_2-A_4)+\lambda^3(A_1A_2+A_4A_2+A_1A_4+b_4b_5\gamma_1\sigma_1+b_5b_6\gamma_2\sigma_2+b_6b_7\gamma_3\sigma_3)+\lambda^2(-A_4b_4b_5\gamma_1\sigma_1\\&-A_4b_5b_6\gamma_2\sigma_2-A_4b_6b_7\gamma_3\sigma_3-A_2b_4b_5\gamma_1\sigma_1-A_1b_5b_6\gamma_2\sigma_2-A_2b_5b_6\gamma_2\sigma_2-A_1b_6b_7\gamma_3\sigma_3-A_1A_2A_4)\\&+\lambda(A_2A_4b_4b_5\gamma_1\sigma_1+A_1A_2b_5b_6\gamma_2\sigma_2+A_1A_4b_5b_6\gamma_2\sigma_2+A_2A_4b_5b_6\gamma_2\sigma_2+A_1A_4b_6b_7\gamma_3\sigma_3+b_4b_5b_6b_7\gamma_1\gamma_3\sigma_3\sigma_1)\\&-A_1A_2A_4b_5b_6\gamma_2\sigma_2-A_4b_4b_5b_6b_7\gamma_1\gamma_3\sigma_1\sigma_3=0,\end{aligned} \tag{51}$$

where $b_4=N_4^*$, $b_5=P^*$, $b_6=Z^*$, $b_7=L^*$, $A_1=-b_5\sigma-\mu_0$, $A_2=b_6\gamma_3-2b_7\sigma_{30}-eq-\mu_3$, $A_3=-(b_7\sigma_4/b_7+d)$, and $A_4=(b_7\gamma_4/b_7+d)-\kappa-\mu_4$. The characteristic Equation (51) can be written as follows:

$$\Delta(\lambda)=a_0\lambda^5+a_1\lambda^4+a_2\lambda^3+a_3\lambda^2+a_4\lambda+a_5=0, \tag{52}$$

where

$$a_0 = 1,$$

$$a_1 = -A_1 - A_2 - A_4,$$

$$a_2 = A_1A_2 + A_4A_2 + A_1A_4 + b_4b_5\gamma_1\sigma_1 + b_5b_6\gamma_2\sigma_2 + b_6b_7\gamma_3\sigma_3,$$

$$a_3 = -A_4b_4b_5\gamma_1\sigma_1 - A_4b_5b_6\gamma_2\sigma_2 - A_4b_6b_7\gamma_3\sigma_3 - A_2b_4b_5\gamma_1\sigma_1 - A_1b_5b_6\gamma_2\sigma_2 - A_2b_5b_6\gamma_2\sigma_2 - A_1b_6b_7\gamma_3\sigma_3 - A_1A_2A_4,$$

$$a_4 = A_2A_4b_4b_5\gamma_1\sigma_1 + A_1A_2b_5b_6\gamma_2\sigma_2 + A_1A_4b_5b_6\gamma_2\sigma_2 + A_2A_4b_5b_6\gamma_2\sigma_2 + A_1A_4b_6b_7\gamma_3\sigma_3 + b_4b_5b_6b_7\gamma_1\gamma_3\sigma_3\sigma_1,$$

$$a_5 = -A_1A_2A_4b_5b_6\gamma_2\sigma_2 - A_4b_4b_5b_6b_7\gamma_1\gamma_3\sigma_1\sigma_3. \quad (53)$$

By the Routh-Hurwitz criterion, it follows that all eigenvalues of the characteristic Equation (52) have negative real parts if

$$a_0 > 0, a_1 > 0, a_1a_2 - a_0a_3 > 0, a_3(a_1a_2 - a_0a_3) - a_1^2a_4 > 0,$$

$$a_1a_3a_4a_2 + a_0a_3a_5a_2 - a_1^2a_4^2 - a_0^2a_5^2 - a_0a_3^2a_4 + 2a_0a_1a_4a_5 - a_1a_5a_2^2 > 0, a_5 > 0. \quad (54)$$

□

Theorem 9. *If the equilibrium $E_* = (N^*, P^*, Z^*, L^*, R^*)$ exists, then, it is locally-asymptotically stable if the conditions in (60) are satisfied.*

Proof. Evaluating the variational matrix at E_* gives

$$J_{E_*} = \begin{pmatrix} -\mu_0 - c_5\sigma_1 & -c_4\sigma_1 & 0 & 0 & 0 \\ c_5\gamma_1 & 0 & -c_5\sigma_2 & 0 & 0 \\ 0 & c_6\gamma_2 & 0 & -c_6\sigma_3 & 0 \\ 0 & 0 & c_7\gamma_3 & -eq + c_6\gamma_3 - \mu_3 - \frac{c_8\sigma_4}{d+c_7} + \frac{c_7c_8\sigma_4}{(d+c_7)^2} - 2c_7\sigma_{30} & -\frac{c_7\sigma_4}{d+c_7} \\ 0 & 0 & 0 & \frac{c_8\gamma_4}{d+c_7} - \frac{c_7c_8\gamma_4}{(d+c_7)^2} & 0 \end{pmatrix}, \quad (55)$$

where $c_4 = N^*$, $c_5 = P^*$, $c_6 = Z^*$, $c_7 = L^*$, and $c_8 = R^*$. (55) simplifies to

$$J_{E_*} = \begin{pmatrix} B_1 - \lambda & -c_4\sigma_1 & 0 & 0 & 0 \\ c_5\gamma_1 & -\lambda & -c_5\sigma_2 & 0 & 0 \\ 0 & c_6\gamma_2 & -\lambda & -c_6\sigma_3 & 0 \\ 0 & 0 & c_7\gamma_3 & B_2 - \lambda & B_3 \\ 0 & 0 & 0 & B_4 & -\lambda \end{pmatrix}, \quad (56)$$

where $B_1 = -c_5\sigma_1 - \mu_0$, $B_2 = c_6\gamma_3 - (c_8\sigma_4/c_7 + d) + (c_7c_8\sigma_4/(c_7+d)^2) - 2c_7\sigma_{30} - eq - \mu_3$, $B_3 = -(c_7\sigma_4/c_7 + d)$, and $B_4 = (c_8\gamma_4/c_7 + d) - (c_7c_8\gamma_4/(c_7+d)^2)$. The eigenvalues of (56) are the roots of the auxiliary equation

$$\det\left(J_{E_*}\right) = 0. \quad (57)$$

The characteristic Equation (57) can be written as follows:

$$\Delta(\lambda) = a_0\lambda^5 + a_1\lambda^4 + a_2\lambda^3 + a_3\lambda^2 + a_4\lambda + a_5 = 0, \quad (58)$$

where

$$\begin{aligned} a_0 &= 1, \\ a_1 &= -B_1 - B_2, \\ a_2 &= B_1B_2 - B_3B_4 + c_4c_5\gamma_1\sigma_1 + c_5c_6\gamma_2\sigma_2 + c_6c_7\gamma_3\sigma_3, \\ a_3 &= -B_2c_4c_5\gamma_1\sigma_1 - B_1c_5c_6\gamma_2\sigma_2 - B_2c_5c_6\gamma_2\sigma_2 - B_1c_6c_7, \\ a_4 &= -B_3B_4c_4c_5\gamma_1\sigma_1 + B_1B_2c_5c_6\gamma_2\sigma_2 - B_3B_4c_5c_6\gamma_2\sigma_2 + c_4c_5c_6c_7\gamma_1\gamma_3\sigma_3\sigma_1, \\ a_5 &= B_1B_3B_4c_5c_6\gamma_2\sigma_2. \end{aligned} \quad (59)$$

By the Routh-Hurwitz criterion, it follows that all eigenvalues of the characteristic Equation (58) have negative real parts if

$$a_0 > 0, a_1 > 0, a_1a_2 - a_0a_3 > 0, a_3(a_1a_2 - a_0a_3) - a_1^2a_4 > 0,$$
$$a_1a_3a_4a_2 + a_0a_3a_5a_2 - a_1^2a_4^2 - a_0^2a_5^2 - a_0a_3^2a_4 + 2a_0a_1a_4a_5 - a_1a_5a_2^2 > 0, a_5 > 0. \quad (60)$$

□

Remark 10. If the conditions for E_* in (60) are not satisfied for a given set of parameter values, then the respective steady state will be unstable, and there is a possibility of oscillatory behavior for model (1).

Theorem 11. *The equilibrium E_* is globally-asymptotically stable if the conditions in (63) are satisfied for the Lyapunov function in (61).*

Proof. The proof follows Lyapunov's second method. Let $N - N^* > 0$, $P - P^* > 0$, $Z - Z^* > 0$, $L - L^* > 0$, $R - R^* > 0$. Let $V(N, P, Z, L, R)$ be a positive Lyapunov function [26, 27], such that $V(N^*, P^*, Z^*, L^*, R^*) = 0$ by,

$$\begin{aligned} V(N,P,Z,L,R) = {} & \beta_1\left(N - N^* - N^*\ln\frac{N}{N^*}\right) \\ & + \beta_2\left(P - P^* - P^*\ln\frac{P}{P^*}\right) \\ & + \beta_3\left(Z - Z^* - Z^*\ln\frac{Z}{Z^*}\right) \\ & + \beta_4\left(L - L^* - L^*\ln\frac{L}{L^*}\right), \\ & + \beta_5\left(R - R^* - R^*\ln\frac{R}{R^*}\right), \end{aligned} \quad (61)$$

where $\beta_i{}'s$, $i = 1, 2, 3, 4, 5$ are positive constants. V is a positive definite function in the set Ψ, except at E_* where it is zero. The rate of change of V along the solution of system (1) is given by

$$\begin{aligned}
\dot{V} &= \beta_1(N-N^*)\frac{\dot{N}}{N} + \beta_2(P-P^*)\frac{\dot{P}}{P} + \beta_3(Z-Z^*)\frac{\dot{Z}}{Z} \\
&\quad + \beta_4(L-L^*)\frac{\dot{L}}{L} + \beta_5(R-R^*)\frac{\dot{R}}{R}, \\
&= -\beta_1(N-N^*)\left[\mu_0 + \sigma_1 P - \frac{a}{N}\right] - \beta_2(P-P^*) \\
&\quad \cdot [\mu_1 + \sigma_2 Z - \gamma_1 N] - \beta_3(Z-Z^*)[\mu_2 + \sigma_3 L - \gamma_2 P] \\
&\quad - \beta_4(L-L^*)\left[\mu_3 + qE + \sigma_{30}L + \frac{\sigma_4 R}{d+L} - \gamma_3 Z\right] \\
&\quad - \beta_5(R-R^*)\left[\kappa\eta + \mu_4 - \frac{\gamma_4 L}{d+L}\right], \\
&= -\beta_1(N-N^*)\left[\mu_0 + \sigma_1 P - \frac{a}{N} - \mu_0 - \sigma_1 P^* + \frac{a}{N^*}\right] \\
&\quad - \beta_2(P-P^*)[\mu_1 + \sigma_2 Z - \gamma_1 N - \mu_1 - \sigma_2 Z^* + \gamma_1 N^*] \\
&\quad - \beta_3(Z-Z^*)[\mu_2 + \sigma_3 L - \gamma_2 P - \mu_2 - \sigma_3 L^* + \gamma_2 P^*] \\
&\quad - \beta_4(L-L^*)\left[\mu_3 + qE + \sigma_{30}L + \frac{\sigma_4 R}{d+L} - \gamma_3 Z - \mu_3 - qE\right. \\
&\quad \left. - \sigma_{30}L^* - \frac{\sigma_4 R^*}{d+L^*} + \gamma_3 Z^*\right] \\
&\quad - \beta_5(R-R^*)\left[\kappa\eta + \mu_4 - \frac{\gamma_4 L}{d+L} - \kappa\eta - \mu_4 + \frac{\gamma_4 L^*}{d+L^*}\right],
\end{aligned}$$

$$\begin{aligned}
\dot{V} &\le -\frac{\beta_1 a}{NN^*}(N-N^*)^2 - (N-N^*)(P-P^*)[\beta_1\sigma_1 - \beta_2\gamma_1] \\
&\quad - (P-P^*)(Z-Z^*)[\beta_2\sigma_2 - \beta_3\gamma_2] - (Z-Z^*)(L-L^*) \\
&\quad \cdot [\beta_3\sigma_3 - \beta_4\gamma_3] - \beta_4\sigma_{30}(L-L^*)^2 - d(L-L^*)(R-R^*) \\
&\quad \cdot [\beta_4\sigma_4 - \beta_5\gamma_4].
\end{aligned} \tag{62}$$

Then, $\dot{V} \le 0$ if

$$\begin{aligned}
&\beta_1\sigma_1 \ge \beta_2\gamma_1, \beta_2\sigma_2 \ge \beta_3\gamma_2, \\
&\beta_3\sigma_3 \ge \beta_4\gamma_3, \beta_4\sigma_4 \ge \beta_5\gamma_4.
\end{aligned} \tag{63}$$

Thus, in the region bounded by all points ($N > N^*$, $P > P^*$, $Z > Z^*$, $L > L^*$, $R > R^*$) in (63),

E_* is globally-asymptotically stable. □

The stability of the periodic solutions is discussed in the bifurcation analysis section.

5. Bifurcation Analysis

The 5D system (1) is written as

$$\dot{x} = F(x, \eta), x \in \mathbb{R}^5, F \in C^\infty, \tag{64}$$

where η is a bifurcation parameter. Bifurcation analysis of model (64) is done using the Hopf bifurcation theorem by Guckenheimer and Holmes [28].

Theorem 12. *Assume that model (64) has the following characteristics*

(1) The model has a smooth equilibria curve

$$F(x_*(\eta), \eta) = 0. \tag{65}$$

(2) The auxiliary equation

$$Q_5(\lambda) = \lambda^5 + \zeta_1\lambda^4 + \zeta_2\lambda^3 + \zeta_3\lambda^2 + \zeta_4\lambda + \zeta_5 = 0, \tag{66}$$

has complex conjugate roots (nonhyperbolicity condition)

$$\lambda_{1,2} = \left(\lambda(\eta_c), \bar{\lambda}(\eta_c)\right) = \left(i\sqrt{\omega}, -i\sqrt{\omega}\right), \omega > 0, \tag{67}$$

and if the condition

$$\Psi = (\zeta_3 - \zeta_1\zeta_2)(\zeta_5\zeta_2 - \zeta_3\zeta_4) - (\zeta_5 - \zeta_1\zeta_4)^2 = 0, \tag{68}$$

with

$$\omega = \frac{\zeta_5 - \zeta_1\zeta_4}{\zeta_3 - \zeta_1\zeta_2} > 0, \tag{69}$$

is satisfied, and there are no other roots with zero real parts and $\lambda_i (i = 3, 4, 5.)$ have nonzero real parts if

$$\zeta_3 - \zeta_1\omega \ne 0, \tag{70}$$

and have negative real parts if

$$\zeta_1 > 0, \zeta_3 - \zeta_1\zeta_2 < 0, \zeta_3 - \zeta_1\omega > 0. \tag{71}$$

(3) The transversality condition

$$\left.\frac{d\Psi(\eta)}{d\eta}\right|_{\eta=\eta_c} \ne 0, \tag{72}$$

is satisfied, and then, there is a Poincare$'$-Andronov-Hopf bifurcation.

6. Numerical Simulations

Numerical simulations of the model system (1) are carried out to investigate the dynamics of the *Limnothrissa miodon* model for the main bifurcation parameter γ_2, using the default parameter values in Equation (73)

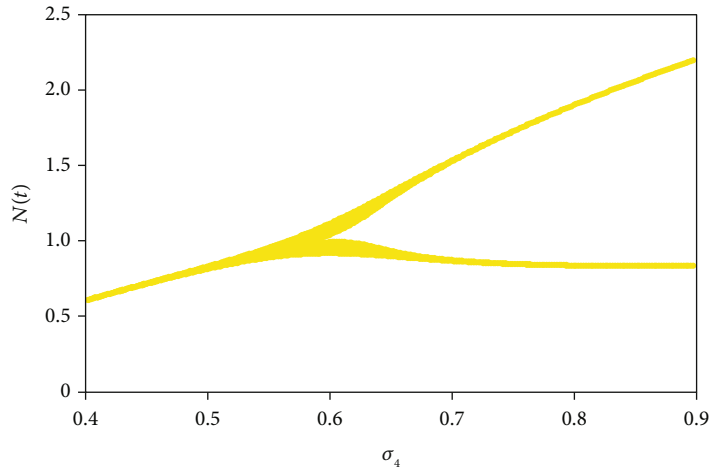

(a)

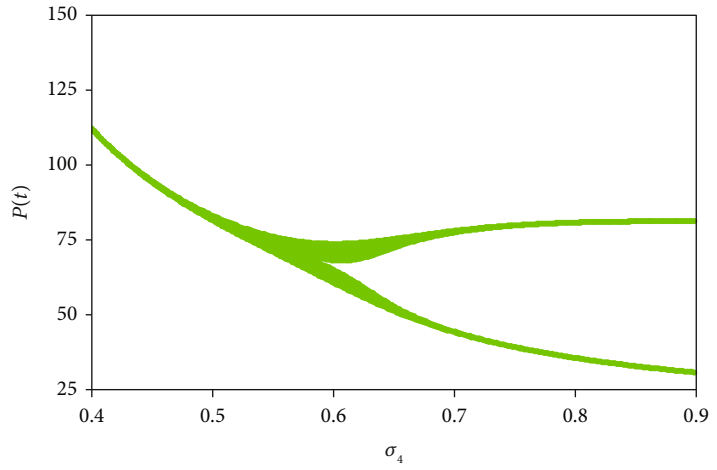

(b)

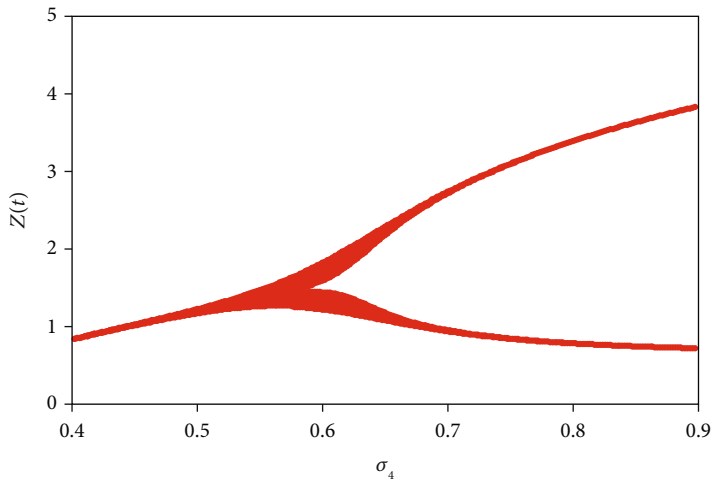

(c)

Figure 2: Continued.

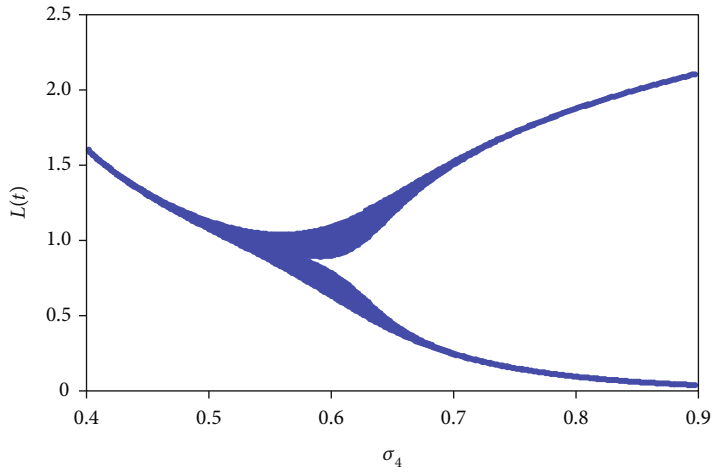

(d)

FIGURE 2: Bifurcation diagram for parameter σ_4 versus (a) nutrients; (b) phytoplankton; (c) zooplankton; and (d) *Limnothrissa miodon* for model system (1) with assumed initial condition: $N(0) = 10, P(0) = 7, Z(0) = 4, L(0) = 2, R(0) = 0.5$ using the default parameter values.

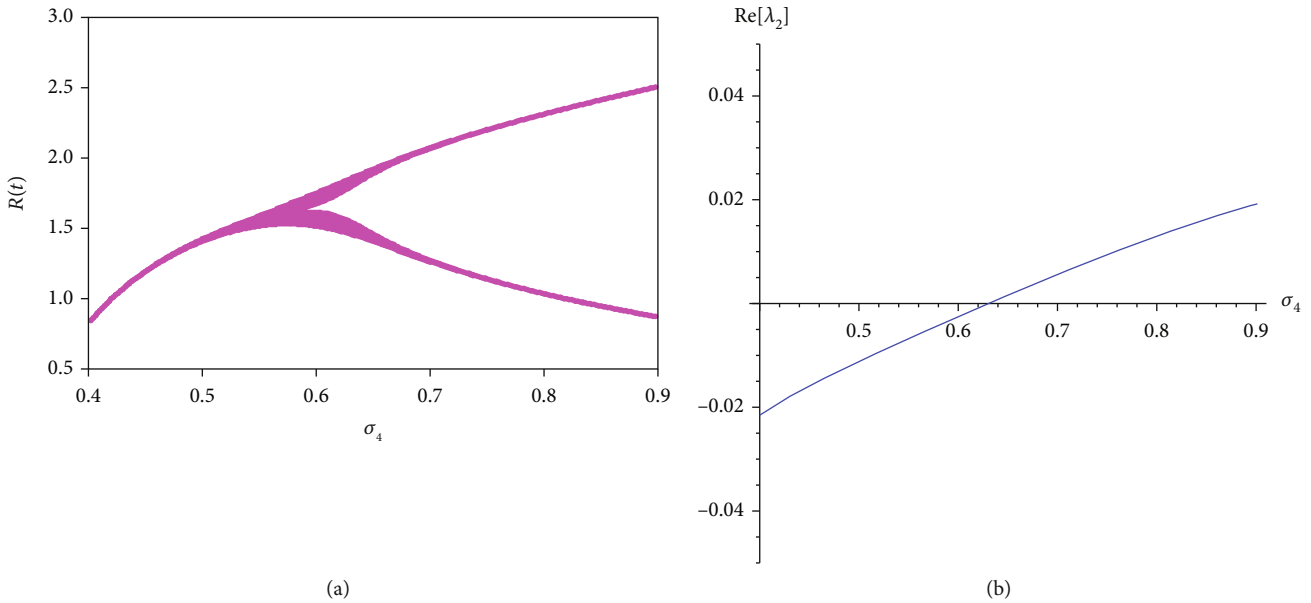

(a) (b)

FIGURE 3: (a) Bifurcation diagram for tigerfish versus σ_4. (b) Plot of real part of eigenvalues of the Jacobian matrix of model (1) for $0.4 \leq \sigma_4 \leq 0.9$.

$$a = 20.3, \mu_0 = 0.0096, \sigma_1 = 0.3, \gamma_1 = 0.3, \mu_1 = 0.032, \sigma_2 = 0.18, \gamma_2 = 0.005,$$
$$\mu_2 = 0.08, \sigma_3 = 0.3, \sigma_{30} = 0.01, \gamma_3 = 0.36, \mu_3 = 0.05, q = 0.00027999, E = 500,$$
$$\kappa\eta = 0.16, \sigma_4 = 0.4, \gamma_4 = 0.4, d = 2, \text{and } \mu_4 = 0.018. \tag{73}$$

The parameter values in Equation (73) are obtained from published data and others are estimates. A fourth-order Runge-Kutta numerical scheme coded in Wolfram Mathematica is used for the numerical simulations. For model system (1), the units of the variables N, P, Z, L, and R are $\mu g l^{-1}$.

6.1. Parameter σ_4. There is no bifurcation for varying σ_4, but a Hopf bifurcation exists for varying σ_4 with $\gamma_4 = \sigma_4$. The predation rate of tigerfish on kapenta is varied from 0.4 to 0.9 with $\gamma_4 = \sigma_4$. Figures 2 and 3(a) show the bifurcation diagrams for the bifurcation parameter σ_4.

The Hopf bifurcation value is 0.63076 for the control parameter σ_4 and is shown in Figure 3(b). From the coefficient criteria in Theorem 12, we obtain $\sigma_4 = \sigma_{4,c} = 0.63076$. Equation (69) gives $\omega = 0.225435, \lambda_{1,2} = \pm i\sqrt{\omega} = \pm 0.4748i$, and $T = (2\pi/\omega) = 27.8714$ days. From Theorem 12, Equation (71), we obtain $\zeta_1 = 18.8633$, $\zeta_3 - \zeta_1\zeta_2 = -79.8152$ and $\zeta_3 - \zeta_1\omega = 0.37348$. The coefficient criteria in Equation (71) are satisfied and therefore showing existence of a simple Hopf bifurcation at the critical value $\sigma_{4,c}$ of the bifurcation parameter σ_4. The transversality condition in Equation (72) of Theorem 12 is satisfied since $d\Psi(\sigma_4)/d\sigma_4|_{\sigma_4=\sigma_{4,c}} = -246.512$. The eigenvalues at $\sigma_{4,c}$ are $\{-18.6363, -0.113515 - 0.08458i,$

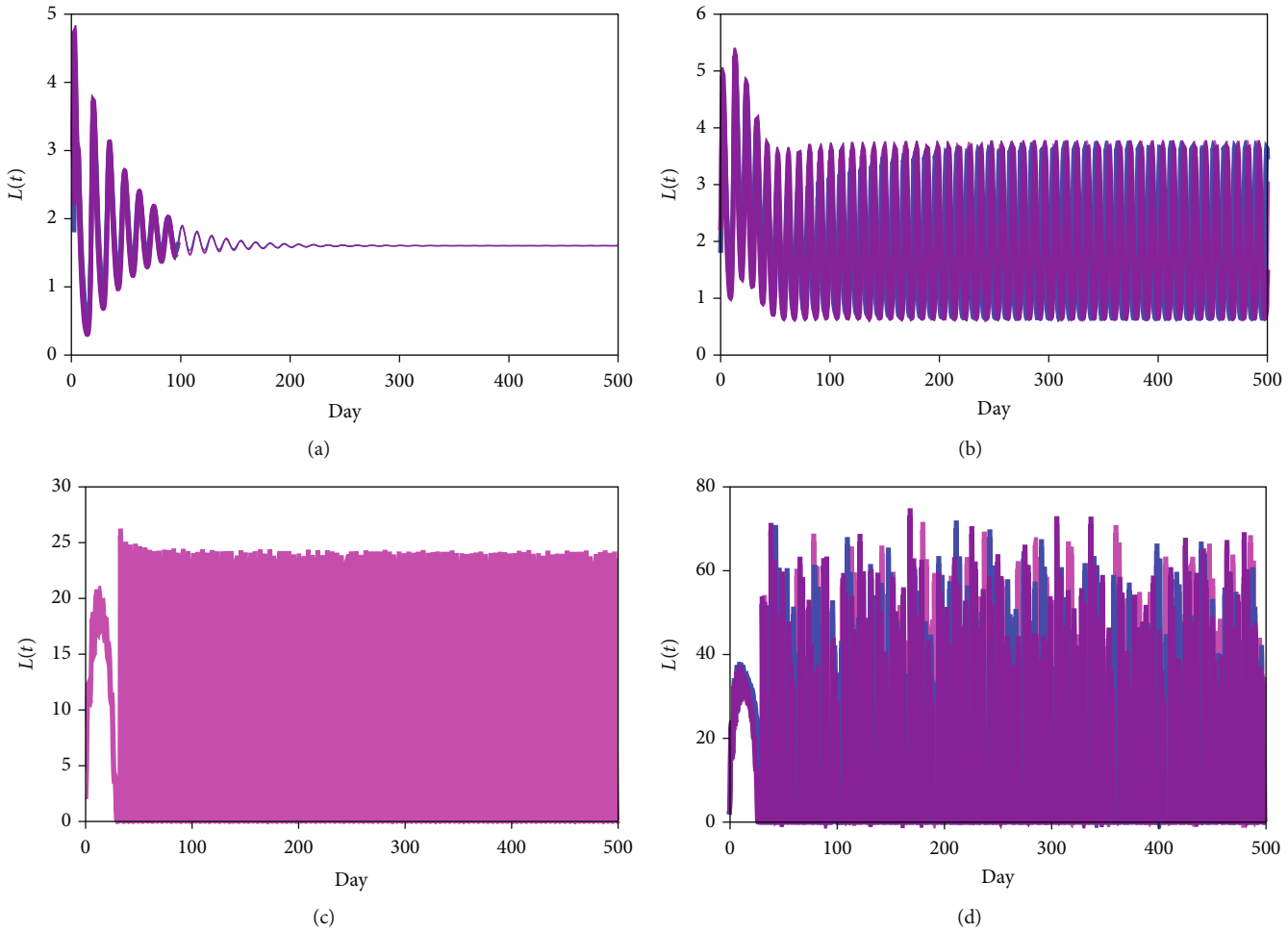

Figure 4: Time series plot of *Limnothrissa miodon* for (a) $\gamma_2 = 0.005$; (b) $\gamma_2 = 0.0095$; (c) $\gamma_2 = 0.075$; and (d) $\gamma_2 = 0.16$ for model (1) with assumed initial condition: $N(0) = 9.8, P(0) = 6.8, Z(0) = 3.8, L(0) = 1.8, R(0) = 0.3$; $N(0) = 10, P(0) = 7, Z(0) = 4, L(0) = 2, R(0) = 0.5$; $N(0) = 10.2, P(0) = 7.2, Z(0) = 4.2, L(0) = 2.2, R(0) = 0.7$, using the default parameter values.

$-0.113515 + 0.084586i, -0.4748i, +0.4748i\}$. The Hopf bifurcation is supercritical since as the bifurcation parameter σ_4 is varied with $\gamma_4 = \sigma_4$ the stable positive interior point loses its stability and a stable periodic orbit simultaneously appears.

Figure 3 shows the effect of varying σ_4 for $0.4 \le \sigma_4 \le 0.9$ with $\sigma_4 = \gamma_4$. The bifurcation results show that there is a decrease in kapenta population density for $0.4 \le \sigma_4 < 0.63076$. Further increase of σ_4 for $0.63076 < \sigma_4 \le 0.9$ results in a period orbit of period 1 with increasing amplitude. Inefficient tigerfish predation on kapenta results in a decrease in the co-existence equilibrium value for kapenta, and efficient predation increases the chance of periodic behavior in the dynamical system. Therefore, the predation rate σ_4, together with the tigerfish growth rate γ_4, significantly determines the nature of the predator-prey relationship between tigerfish and kapenta. Simulation results show no chaotic behavior for the bifurcation control parameter σ_4.

6.2. Parameter γ_2. The interior equilibrium, $E_* = (0.602831, 112.216, 0.82694, 1.6036, 0.825832)$ for model (1), with damped oscillations for the set of default parameters are shown in Figure 4(a) for *Limnothrissa miodon* and 5(a) for zooplankton, *Limnothrissa miodon*, and tigerfish.

The positive interior equilibrium E_* for model system (1) is permanent for the set of default parameter values. For the main bifurcation parameter, model (1) bifurcates into a limit cycle of period 1 at $\gamma_{2,c} = 0.00818058$. Time series plots and phase portraits for $\gamma_2 = 0.0095$ are shown in Figures 4(b) and 5(b). Time series plots and phase portraits for $\gamma_2 = 0.075$ are shown in Figures 4(c) and 5(c). The phase portraits show periodic doubling. Time series plots and phase portraits for $\gamma_2 = 0.16$ are shown in Figures 4(d) and 5(d). The phase portraits show a chaotic attractor at $\gamma_2 = 0.16$. Varying the zooplankton growth rate γ_2 results in some interesting dynamics for model (1). The stability of model (1) changes from a stable coexistence equilibrium into a stable periodic orbit and then periodic doubling enroute to chaos. Therefore, we can conclude that γ_2 plays an important role in the dynamics of model (1). The trajectories in Figures 4 and 5 are aperiodic as they are showing erratic behavior. The irregular fluctuations can be attributed to the nonlinearity of the model (1). By visual inspection of the phase portraits in Figures 4(d) and 5(d) and from the magnitude of the maximal Lyapunov exponent, 0.107838, it can be seen that the trajectories are sensitive to initial

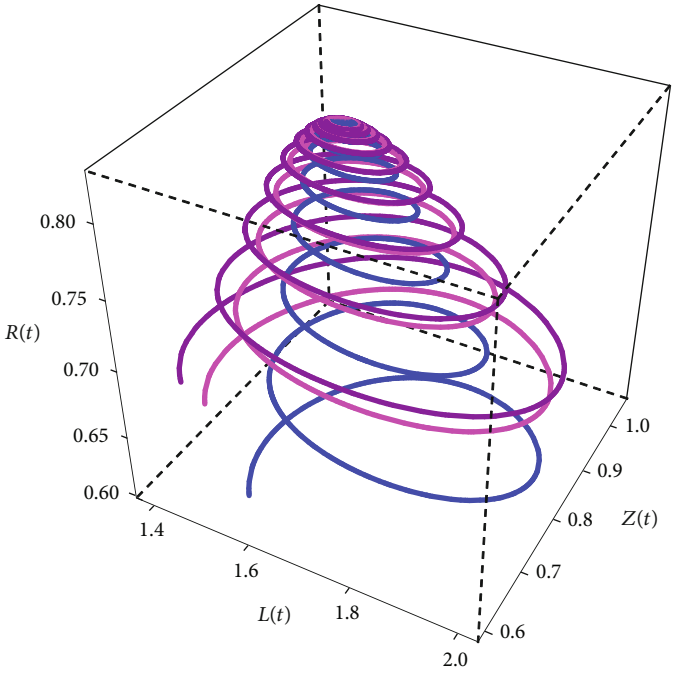

(a)

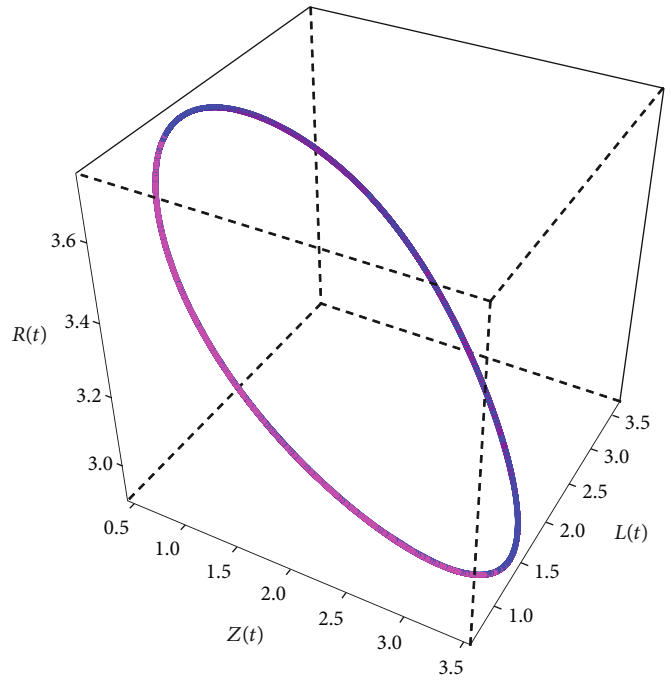

(b)

Figure 5: Continued.

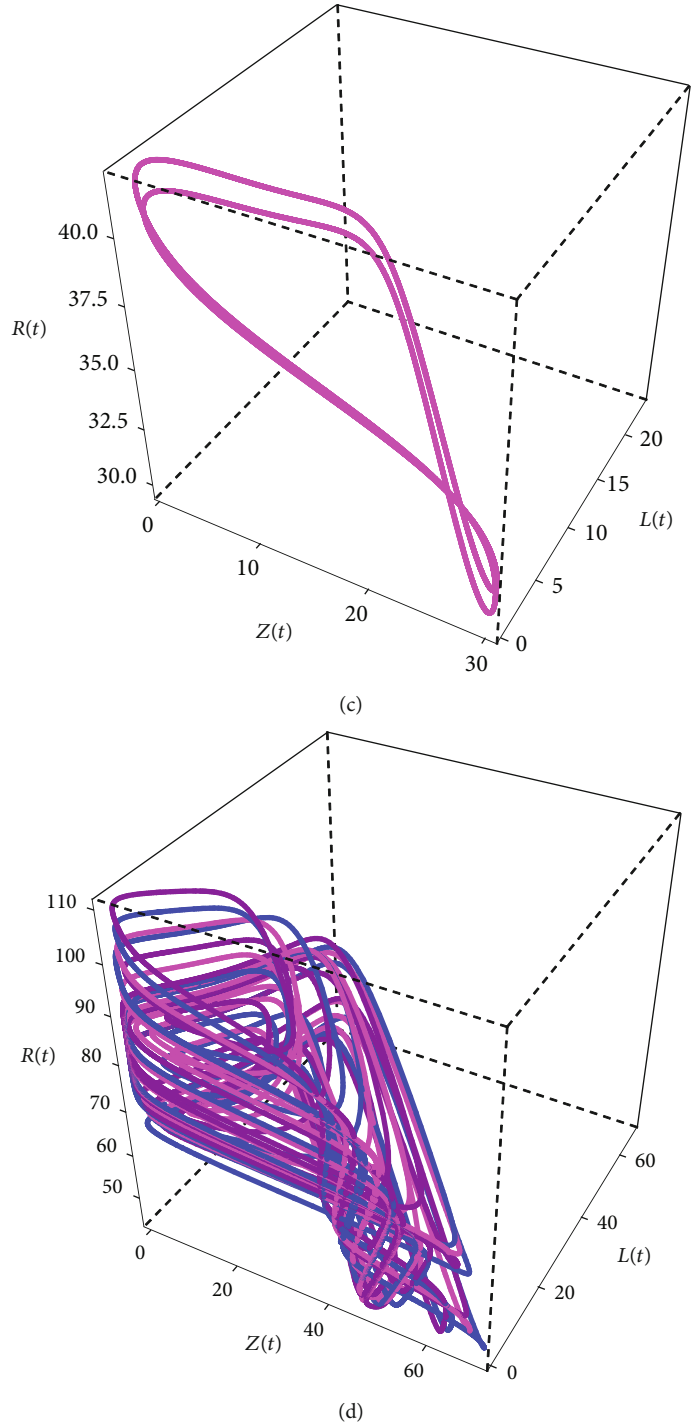

FIGURE 5: Phase portrait of zooplankton, *Limnothrissa miodon* and tigerfish (a) $\gamma_2 = 0.005$, (b) $\gamma_2 = 0.0095$, (c) $\gamma_2 = 0.075$, and (d) $\gamma_2 = 0.16$ for model (1) with assumed initial condition: $N(0) = 9.8, P(0) = 6.8, Z(0) = 3.8, L(0) = 1.8, R(0) = 0.3$ (time series with blue color); $N(0) = 10, P(0) = 7, Z(0) = 4, L(0) = 2, R(0) = 0.5$ (time series with magenta color); $N(0) = 10.2, P(0) = 7.2, Z(0) = 4.2, L(0) = 2.2, R(0) = 0.7$ (time series with purple color), using the default parameter values.

conditions and, therefore, it is impossible to predict the long-term behavior of model system (1) for $\gamma_2 = 0.16$. The trajectories are random and bounded in phase space and they converge to a strange attractor, which has a complex (fractal) geometric structure.

We use the Hopf bifurcation theorem by Guckenheimer and Holmes [28] together with conditions by Douskos and Markellos [29] to characterize the bifurcation of the 5D model (1). For the main control bifurcation parameter γ_2, we obtain the auxiliary equation

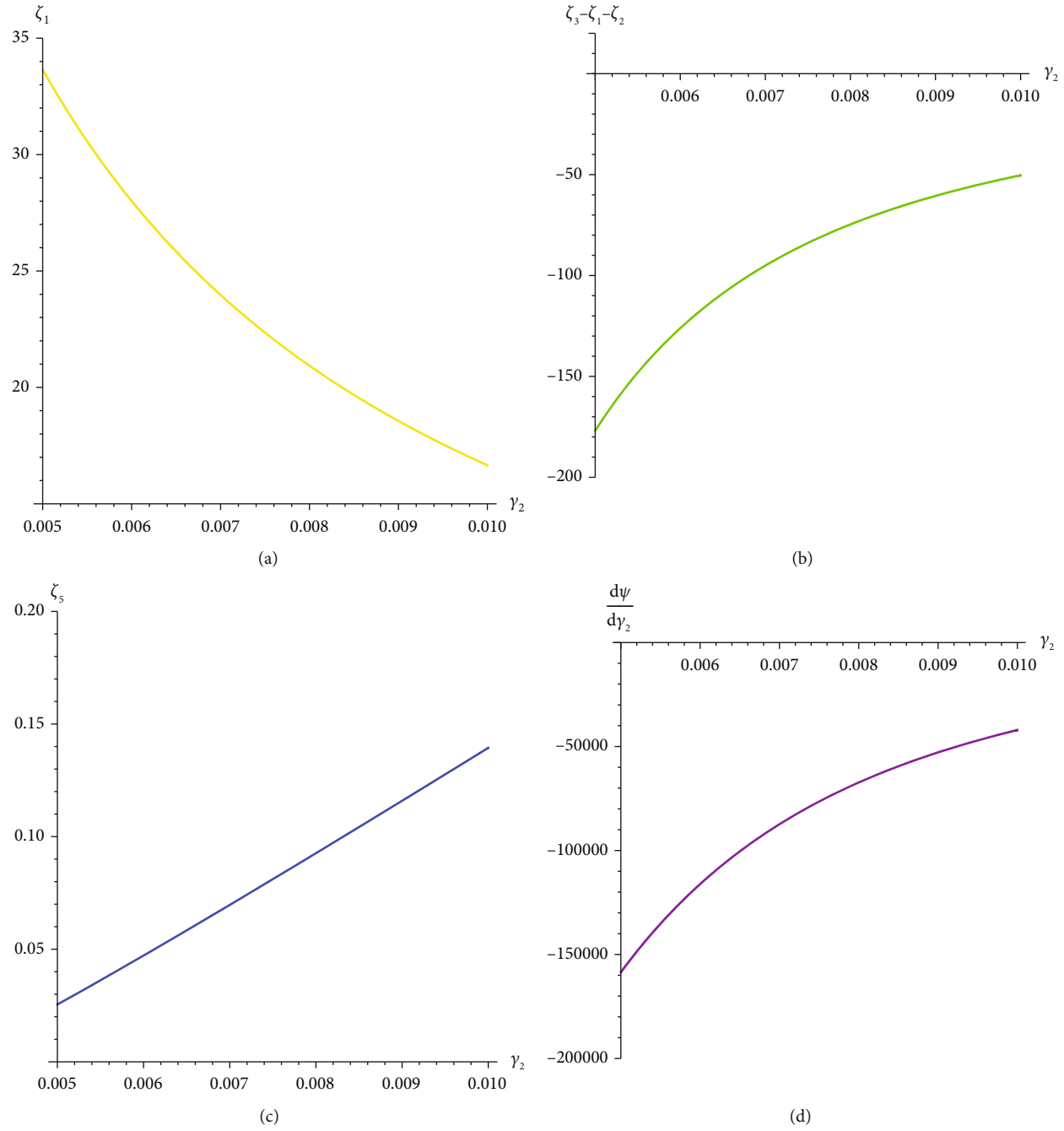

FIGURE 6: Plots for parameter γ_2 versus (a) ζ_1; (b) $\zeta_3 - \zeta_1\zeta_2$; (c) $\zeta_3 - \zeta_1\omega$; and (d) $d\Psi(\gamma_2)/d\gamma_2$ for model system (1) with assumed initial condition: $N(0) = 10, P(0) = 7, Z(0) = 4, L(0) = 2, R(0) = 0.5$ using the default parameter values in (73).

$$Q_5(\lambda) = \lambda^5 + \zeta_1\lambda^4 + \zeta_2\lambda^3 + \zeta_3\lambda^2 + \zeta_4\lambda + \zeta_5 = 0, \quad (74)$$

where $\zeta_1 = A_1/A_0$; $\zeta_2 = A_2/A_0$; $\zeta_3 = A_3/A_0$; $\zeta_4 = A_4/A_0$; and $\zeta_5 = A_5/A_0$, and

$$A_0 = -1.\gamma_2^5 - 70.1351\gamma_2^4 - 1844.6\gamma_2^3 - 21561.9\gamma_2^2 - 94515.4\gamma_2,$$

$$A_1 = 564.448\gamma_2^5 + 29688.\gamma_2^4 + 520444.\gamma_2^3 + 3.03997 \times 10^6\gamma_2^2 - 17409.7\gamma_2 - 15909.2,$$

$$A_2 = -1086.15\gamma_2^5 - 57143.6\gamma_2^4 - 1.00231 \times 10^6\gamma_2^3 - 5.86456 \times 10^6\gamma_2^2 - 56805.4\gamma_2 - 2166.84,$$

$$A_3 = 200890.\gamma_2^5 + 7.1036 \times 10^6\gamma_2^4 + 6.38216 \times 10^7\gamma_2^3 + 1.79792 \times 10^7\gamma_2^2 - 1.06833 \times 10^6\gamma_2 + 1199.88,$$

$$A_4 = -42672.5\gamma_2^5 - 1.54096 \times 10^6\gamma_2^4 - 1.4681 \times 10^7\gamma_2^3 - 1.36957 \times 10^7\gamma_2^2 - 20141.7\gamma_2 + 38.9047,$$

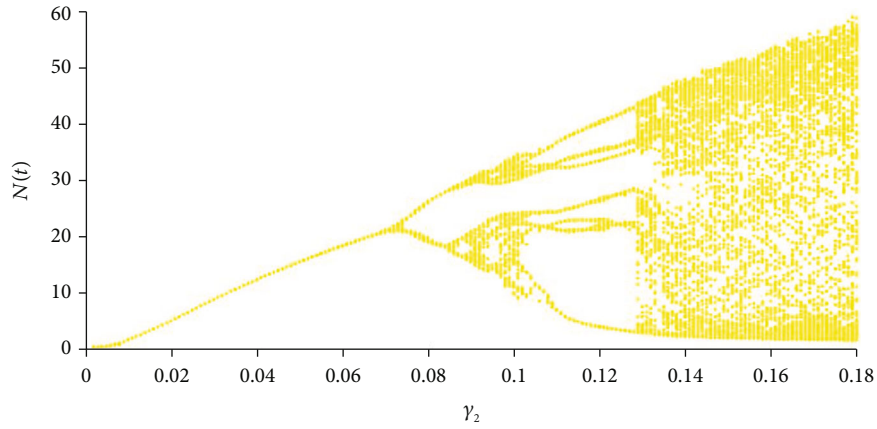

(a)

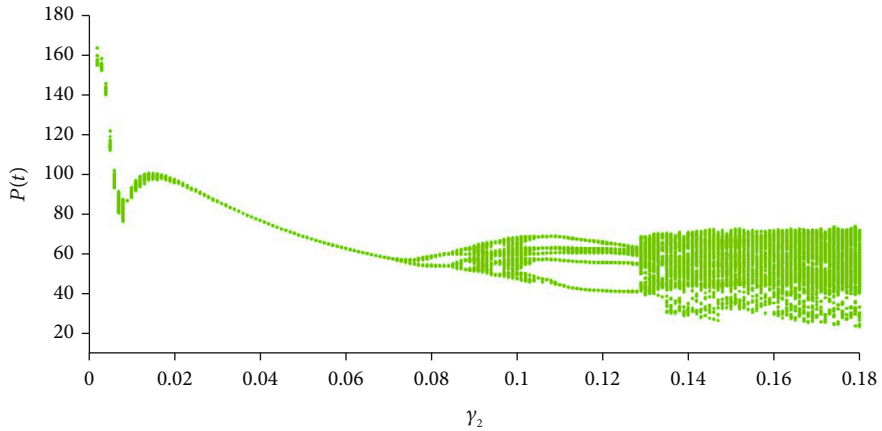

(b)

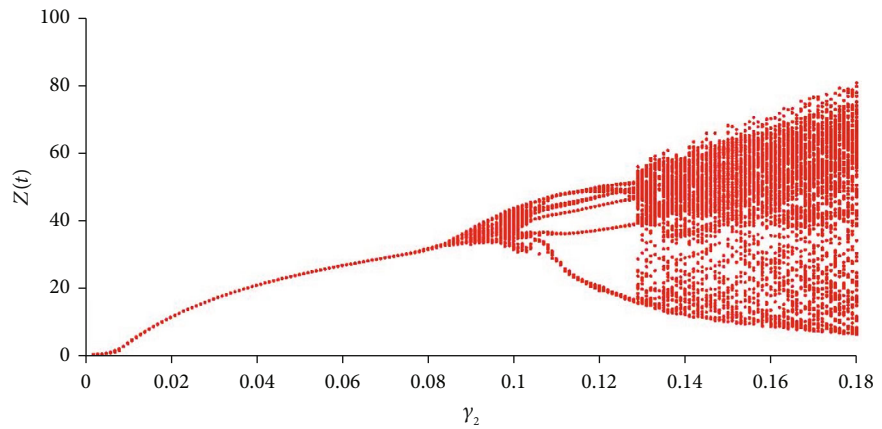

(c)

Figure 7: Continued.

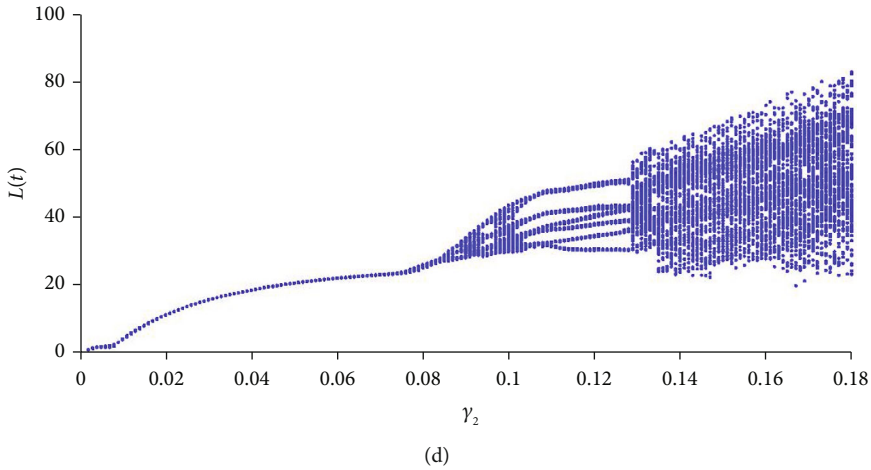

FIGURE 7: Bifurcation diagram for parameter γ_2 versus (a) nutrients; (b) phytoplankton; (c) zooplankton; and (d) *Limnothrissa miodon* for model system (1) with assumed initial condition: $N(0) = 10, P(0) = 7, Z(0) = 4, L(0) = 2, R(0) = 0.5$ using the default parameter values in (73).

$$A_5 = -428.171\gamma_2^5 - 22520.4\gamma_2^4 - 394799.\gamma_2^3 - 2.30622 \times 10^6\gamma_2^2 + 10655.1\gamma_2 - 7.61994. \quad (75)$$

Using the coefficient criteria of Hopf bifurcations without using eigenvalues and solving Equation (68) numerically for the bifurcation parameter γ_2 in Wolfram Mathematica 11, we obtain $\gamma_2 = \gamma_{2,c} = 0.00818058$. Equation (69) gives $\omega = 0.385339, \lambda_{1,2} = \pm i\sqrt{\omega} = \pm 0.620757i$, and $T = (2\pi/\omega) = 16.3056$ days. From Theorem 5.8, Equation (71), we obtain $\zeta_1 = 20.4586$, $\zeta_3 - \zeta_1\zeta_2 = -71.7456$, and $\zeta_3 - \zeta_1\omega = 0.251287$. The plots of γ_2 versus ζ_1, $\zeta_3 - \zeta_1\zeta_2$, and ζ_5 are shown in Figures 6(a)–6(c), respectively. The coefficient criteria in Equation (71) are satisfied and therefore showing existence of a simple Hopf bifurcation at the critical value $\gamma_{2,c}$ of the bifurcation parameter γ_2. The transversality condition is satisfied since $d\Psi(\gamma_2)/d\gamma_2|_{\gamma_2=\gamma_{2,c}} = -64347.8$ and Figure 6(d) show that for $0.005 \le \gamma_2 \le 0.01$, the condition in Equation (72) of Theorem 5.9 is satisfied. The Hopf bifurcation is supercritical since as the bifurcation parameter γ_2 is varied, the stable positive interior point loses its stability, and a stable limit cycle simultaneously appears.

Bifurcation diagrams for model (1) were plotted using MATLAB R2016a code. ODE45 solver, which is based on an explicit Runge-Kutta ((4), (5)) formula and the Dormand-Prince method, was used for the numerical solution of the ordinary differential equations in (1). The bifurcation diagrams in Figures 7 and 8(a) show the change in stability for model (1) from a positive interior equilibrium into a limit cycle and period-doubling enroute to chaos for the control parameter, $0 < \gamma_2 \le 0.18$. The zooplankton growth rate parameter γ_2, therefore, has a tremendous effect on the dynamics of model system (1).

For the 5D system in Equation (64), a local Hopf bifurcation occurs at $(x_*(\eta_c), \eta_c)$ if the Jacobian, $J_{F(x_*(\eta_c),\eta_c)}$, has a pair of imaginary roots. Using eigenvalues obtained from $J_{F(x_*(\eta_c),\eta_c)}$, we plot the real part (Re) of the eigenvalues $(\lambda_i$ $(i = 1, 2, 3, 4, 5.))$ against the bifurcation parameter and find the bifurcation point where the curve crosses the axis of the bifurcation parameter as this is where the real part of an eigenvalue of an equilibrium passes through zero. The set of eigenvalues of $J_{F(x_*(\gamma_{2,c}),\gamma_{2,c})}$ are shown in the complex plane in Figure 9(a). The Hopf bifurcation occurs at the point where $\text{Re}(\lambda) = 0$. Using the FindRoot command in Wolfram Mathematica 11, which searches for a numerical root starting from some initial root, the bifurcation value for the control parameter γ_2 is 0.00818058 and is shown in Figure 9(b). Model (1) loses its stability whenever $\gamma_2 > 0.00818058$ for the default set of parameter values. The coexistence equilibrium enters into a Hopf bifurcation at $\gamma_2 = 0.00818058$. The eigenvalues at $\gamma_{2,c}$ are $\{-20.2857, -0.0864343 - 0.0701176i, -0.0864343 + 0.0701176i, -0.620757i, +0.620757i\}$; therefore, the stable coexistence equilibrium bifurcates into a stable periodic orbit.

The Lyapunov spectrum of model system (1) consists of 5 eigenvalues $(\lambda_j, j = 1, 2, 3, 4, 5)$ called Lyapunov exponents. The rate of separation of infinitesimally close trajectories can be characterized by λ_j. The Lyapunov spectrum for model (1) is found using code in Wolfram Mathematica 11 and is shown in Figures 10 and 11.

The Lyapunov exponents for model (1) with $\gamma_2 = 0.055$ and $\gamma_2 = 0.095$ are (-0.0256886, -0.0426366, -0.0563857, -0.0809535, and -34.1637) and (0.000382075, -0.0373874, -0.0946365, -0.103307, and -20.1639) which correspond to the positive interior equilibrium and the limit cycle, respectively. The largest Lyapunov exponent for the model with $\gamma_2 = 0.055$ is less than zero, indicating that nearby trajectories converge, and therefore, the interior equilibrium is a stable fixed point. For $\gamma_2 = 0.095$, the maximal Lyapunov exponent is equal to zero, meaning that nearby trajectories converge to a closed orbit, and therefore, the periodic orbit (limit cycle) is stable.

The Lyapunov exponents for model (1) with $\gamma_2 = 0.16$ are (0.107838, -0.0039426, -0.0135559, -0.190155, and -5.87422). The maximal Lyapunov exponent is $\lambda_1 = 0.107838$, and since $\lambda_1 > 0$, this is an indication of

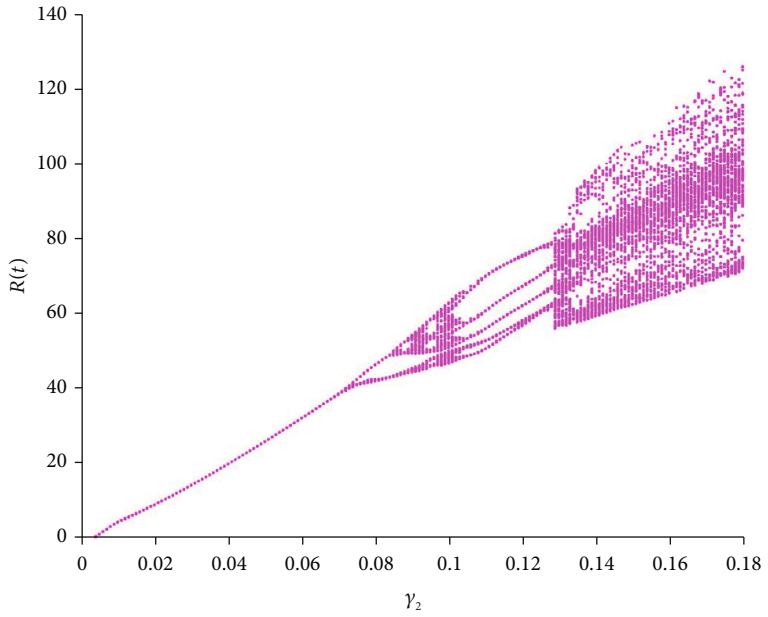

FIGURE 8: Bifurcation diagram for tigerfish versus γ_2 of model (1) for $0 < \gamma_2 \leq 0.18$ and other default parameter values and with assumed initial condition: $N(0) = 10, P(0) = 7, Z(0) = 4, L(0) = 2, R(0) = 0.5$.

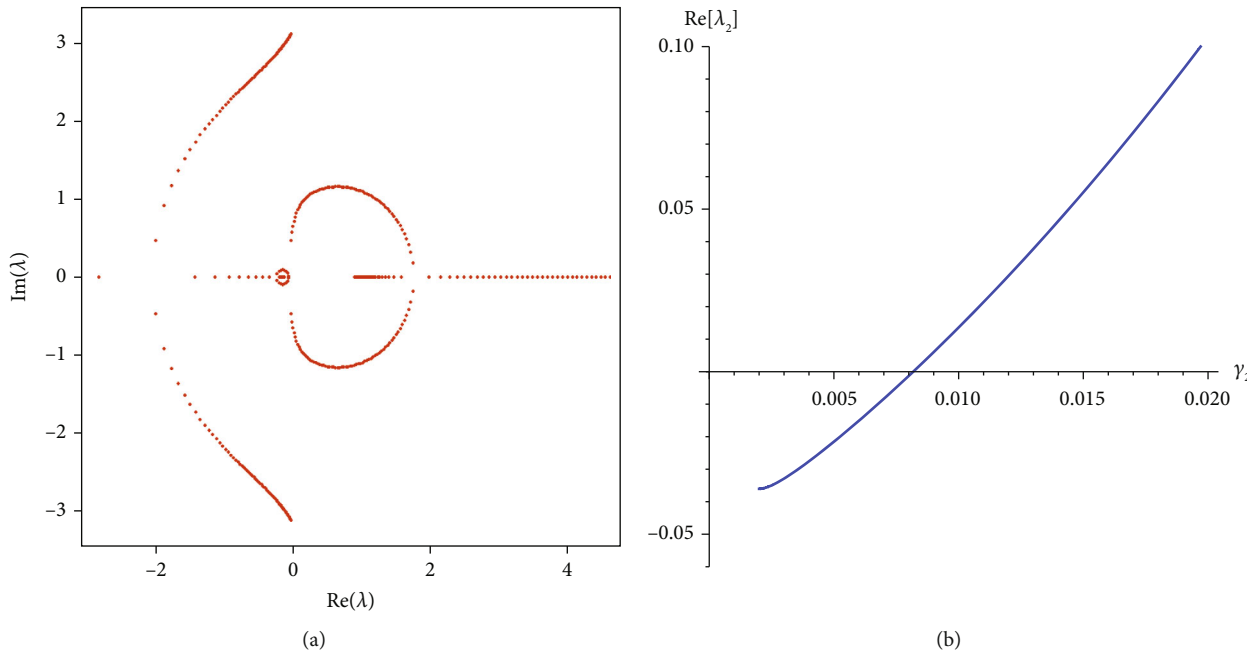

FIGURE 9: (a) Complex plane for $0.002 \leq \gamma_2 \leq 0.18$. (b) Plot of real part of the eigenvalue λ_2 of the Jacobian matrix of model (1) for $0.002 \leq \gamma_2 \leq 0.02$.

divergence of nearby trajectories, and therefore, the dynamical system (1) is unstable and chaotic at $\gamma_2 = 0.16$. For the dynamical system (1), a strange attractor exists in phase space at $\gamma_2 = 0.16$.

7. Conclusions

In this paper, we formulated and analyzed a *Limnothrissa miodon* model with *Hydrocynus vittatus* predation. Positivity and existence of solutions for the model were shown. Local stability analysis results agree with the numerical simulations in that the coexistence equilibrium is locally stable provided that certain conditions are satisfied. The coexistence equilibrium is globally stable if certain conditions are met. In bifurcation analysis, the Hopf bifurcation theorem together with certain conditions for a 5D system was used to find the bifurcation point, angular frequency, period, pair of imaginary eigenvalues, stability, and direction for a

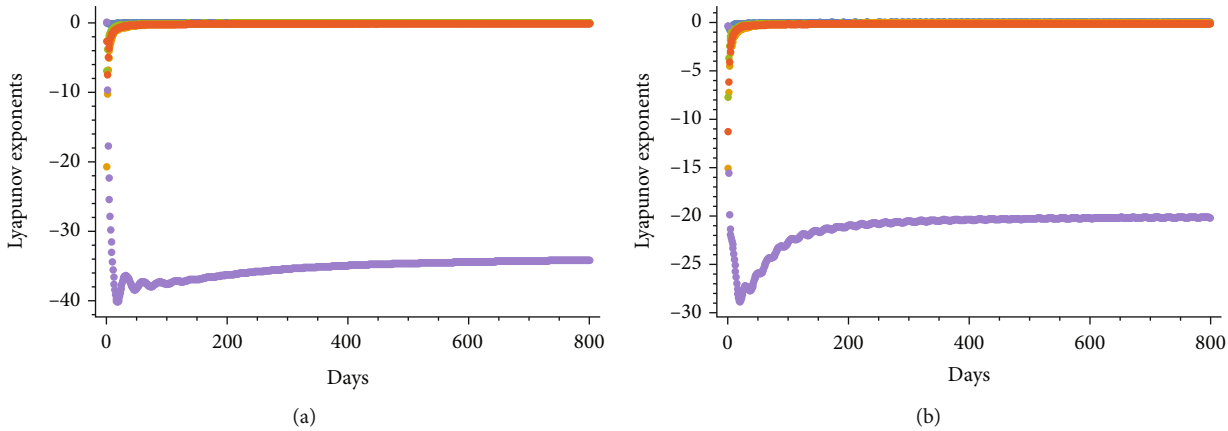

FIGURE 10: Lyapunov spectrum for model (1) for (a) $\gamma_2 = 0.055$; (b) $\gamma_2 = 0.095$ and other default parameter values and with assumed initial condition: $N(0) = 10, P(0) = 7, Z(0) = 4, L(0) = 2, R(0) = 0.5$.

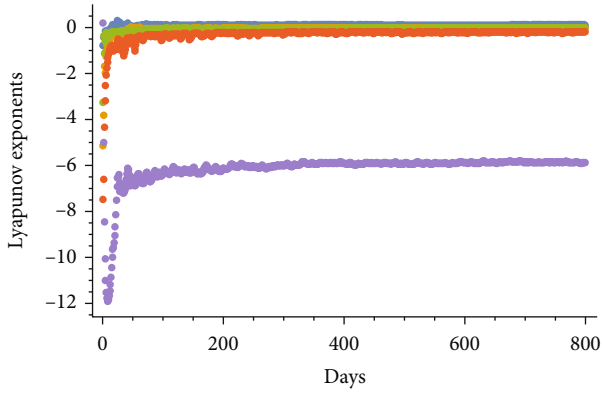

FIGURE 11: Lyapunov spectrum for model (1) for $\gamma_2 = 0.16$ and other default parameter values and with assumed initial condition: $N(0) = 10, P(0) = 7, Z(0) = 4, L(0) = 2, R(0) = 0.5$.

bifurcation control parameter. The eigenvalue method was also used to find the bifurcation point of a bifurcation control parameter. Results from the Hopf bifurcation theorem and from the eigenvalue method for the 5D system were the same. Therefore, either method can be used to find the bifurcation point for a given control parameter for the 5D system. The model changes in stability from a positive interior equilibrium to a limit cycle and period-doubling enroute to chaos for the zooplankton growth rate control parameter, indicating that zooplankton growth rate has a tremendous effect on the dynamics of the model. Therefore, a variation in the zooplankton growth rate can significantly alter the dynamics of *Limnothrissa miodon* in Lake Kariba. The Lyapunov spectrum of exponents was used to show the convergence or divergence of nearby trajectories and to check for the existence of chaos in the aquatic environment. A supercritical simple Hopf bifurcation exists for varying the biological *Hydrocynus vittatus* predation on *Limnothrissa miodon* parameter only if the parameter is equal to the *Hydrocynus vittatus* growth rate coefficient. *Hydrocynus vittatus* predation on *Limnothrissa miodon* changes a stable coexistence equilibrium into a stable periodic orbit if the predation rate coefficient is the same as the *Hydrocynus vittatus* growth rate coefficient. We therefore conclude that *Hydrocynus vittatus* predation on *Limnothrissa miodon* significantly alters the dynamics of *Limnothrissa miodon* whenever the *Hydrocynus vittatus* predation rate coefficient is the same as the *Hydrocynus vittatus* growth rate coefficient. Hopf bifurcation for varying a predation rate coefficient and the Hopf bifurcation leading to chaos for the zooplankton growth rate control parameter is in agreement with findings from other authors. The periodic orbit obtained in bifurcation analysis reflects what actually happens in Lake Kariba as evidenced from actual data shown in Figure 5.1, which shows the cyclical behavior of the *Hydrocynus vittatus* bycatch and *Limnothrissa miodon* catch. Therefore, the Hopf bifurcation results reflect what really happens in the Lake Kariba kapenta fishery. Bifurcation results show that a higher zooplankton growth rate, which implies efficient grazing on phytoplankton, increases the chance of chaos in the dynamical system. Inefficient grazing of phytoplankton by zooplankton implies a lower zooplankton growth rate resulting in simple dynamics in the model system. Therefore, the phytoplankton-zooplankton oscillations and the nature of the zooplankton predation play an important role in model dynamics. An increase in the parameter γ_2 leads to destabilization of the dynamical system (1). The chaotic solutions for model system (1) for the bifurcation parameter γ_2 could not be validated with actual data for nutrients, phytoplankton, zooplankton, kapenta, and tigerfish from the Lake Kariba kapenta fishery, since the sample size of the data available is small and the data was collected at irregular time intervals. Therefore, the unavailability of data is a limitation in validating the deterministic chaos results for the bifurcation control parameter γ_2. In certain ecological systems, chaotic dynamics are expected to contribute to the unpredictability and irregularity of ecological time series [30]. It is debatable whether or not this chaotic behavior observed in Figures 4(d) and 5(d) occurs in the kapenta fishery. The fundamental issue stems from the fact that in most ecological systems, there is a strong stochastic disturbance from environmental factors such as temperature and weather, and this

makes determining whether the irregular structure in the data is due to chaotic dynamics or stochastic perturbations difficult [30]. Phytoplankton dynamics usually show erratic and eruptive "busts and blooms" and have similar characteristics of deterministic chaos [31]. According to Stone and Ezrati [32], it is reasonable to have oscillating and chaotic dynamics in nonlinear deterministic ecological systems with growth processes that are strong and without neglecting the possibility of stochastic processes influencing the variability which arises in nature. For future studies, we intend to model the dynamics of *Limnothrissa miodon* with lake water temperature.

Data Availability

The data used to support the findings in this study are included in the article.

Conflicts of Interest

There are no conflicts of interest for the authors of this study.

Acknowledgments

We are most grateful to staff at the Lake Kariba Fisheries Research Institute and the University of Zimbabwe Lake Kariba Research Station for the provision of data used in this study. Special thanks are due to Dr. Nobuhle Ndlovu, Ms. Adroid T. Chakandinakira, and Ms. P Chirozva. This study was supported by the National University of Science and Technology, Research Board Grant number RDB/90/18.

References

[1] G. Bell-Cross and B. Bell-Cross, "Introduction of Limnothrissa miodon and Limnocaridina tanganicae from Lake Tanganyika into Lake Kariba," *Fisheries Research Bulletin Zambia*, vol. 5, pp. 207–214, 1971.

[2] B. G. Donnelly, *The fish population changes on Lake Kariba between 1960 and 1968*, Part II. Characidae and Atharinidae, Lake Kariba Fisheries Research Institute, 1971.

[3] S. A. Mitchell, "The marginal fish fauna of Lake Kariba," *Kariba Studies*, vol. 8, pp. 109–162, 1976.

[4] G. Bell-Cross, *The Fishes of Rhodesia*, Salisbury, National Museums and Monuments of Rhodesia, 1976.

[5] H. Matthes, "The food and feeding habits of tigerfish, Hydrocynus vittatus (Castelanau 1861), in Lake Kariba," *Beaufortia*, vol. 15, article 143153, 1968.

[6] D. H. S. Kenmuir, "Some aspects of Hydrocynus vittatus Castelnau (tigerfish) research at Lake Kariba," *Newsletter of the Limnological Society of South Africa*, vol. 17, pp. 33–38, 1971.

[7] W. Mhlanga, "Food and feeding habits of tigerfish, Hydrocynus vittatus," in *Lake Kariba, Zimbabwe*, M. L. D. Palomares, B. Samb, T. Diouf, J. M. Vakily, and D. Pauly, Eds., vol. 14, p. 281, Fish biodiversity: local studies as basis for global inferences ACP-EU Fisheries Research Report, 2003.

[8] L. Marufu, T. Dalu, C. Phiri, and T. Nhiwatiwa, "Diet composition changes in tigerfish of Lake Kariba following an invasion by redclaw crayfish," *Annales de Limnologie-International Journal of Limnology*, vol. 53, pp. 47–56, 2017.

[9] W. Mhlanga, "A study of Hydrocynus vittatus. Castelnau in Lake Kariba," *Zimbabwe. African Journal of Tropical Hydrobiology and Fisheries*, vol. 9, no. 1&2, pp. 25–35, 2000.

[10] E. K. Balon and A. G. Coche, "Total production, available production and yield of major fish taxa from Lake Kariba," in *Lake Kariba*, E. K. Balon and A. G. Coche, Eds., vol. 24 of Monographiae Biologicae, pp. 428–445, Springer, Dordrecht, 1974.

[11] J. D. Langerman, *Optimum harvest strategies for tigerfish in Lake Kariba Zimbabwe, [M.S. thesis]*, University of Witwatersrand, Johannesburg, 1984.

[12] B. E. Marshall, "Growth and mortality of the introduced Lake Tanganyika clupeid, Limnothrissa miodon, in Lake Kariba," *Journal of Fish Biology*, vol. 31, no. 5, pp. 603–615, 1987.

[13] M. Takano and S. P. Subramaniam, *Some observations on the predatory feeding habits of Hydrocynus vittatus Castelnau in Lake Kariba*, CIFA Occasional Paper (FAO), 1988.

[14] S. Pal and A. Chatterjee, "Dynamics of the interaction of plankton and planktivorous fish with delay," *Cogent Mathematics*, vol. 2, no. 1, article 1074337, 2015.

[15] S. N. Raw, B. Tiwari, and P. Mishra, "Analysis of a plankton–-fish model with external toxicity and nonlinear harvesting," *Ricerche di Matematica*, vol. 69, pp. 653–681, 2019.

[16] P. Panja and D. K. Jana, "A novel prey-predator quadratic harvesting model via optimal control theory and Hopf bifurcation," *Nepal Journal of Mathematical Sciences*, vol. 1, pp. 1–22, 2021.

[17] L. Madamombe, *The economic development of the kapenta fishery Lake Kariba (Zimbabwe/Zambia), [M.S. thesis]*, Universitetet i Tromsø, Norway, 2002.

[18] B. E. Marshall, "The influence of river flow on pelagic sardine catches in Lake Kariba," *Journal of Fish Biology*, vol. 20, no. 4, pp. 465–469, 1982.

[19] P. Chipungu, *Review of draft proposal for the management of the Zambian inshore fisheries on Lake Kariba*, SADC Fisheries, Zambia-Zimbabwe, 1993.

[20] G. F. Losse, *The small scale fishery on Lake Kariba in Zambia*, CABI, 1998.

[21] M. R. Ndebele-Murisa, *An analysis of primary and secondary production in Lake Kariba in a changing climate, [Ph.D. thesis]*, University of the Western Cape, Bellville, South Africa, 2011.

[22] L. Kinadjian, C. Mwula, K. Nyikahadzoi, and N. Songore, *Bioeconomic Modelling of Kapenta Fisheries on Lake Kariba. Report/Rapport: SFFAO/2014/22*, FAO-Smart Fish Programme of the Indian Ocean Commission, Ebene, Mauritius, 2014.

[23] F. K. Mutasa, B. Jones, and S. D. Hove-Musekwa, "Modelling and analysis of Limnothrissa miodon population in a Lake," *Chaos, Solitons and Fractals*, vol. 136, 2020.

[24] C. S. Holling, "The components of predation as revealed by a study of small mammal predation of the European pine sawfly," *Canadian Entomologist*, vol. 91, no. 5, pp. 293–320, 1959.

[25] R. K. Upadhyay and S. R. Iyengar, *Introduction to mathematical modeling and chaotic dynamics*, Chapman and Hall/CRC, 2013.

[26] A. Korobeinikov, "Lyapunov functions and global stability for SIR and SIRS epidemiological models with non-linear transmission," *Bulletin of Mathematical Biology*, vol. 68, no. 3, pp. 615–626, 2006.

[27] P. Panja, S. Jana, and S. K. Mondal, "Effects of additional food on the dynamics of a three species food chain model incorporating refuge and harvesting," *International Journal of Nonlinear Sciences and Numerical Simulation*, vol. 20, no. 7-8, pp. 787–801, 2019.

[28] J. Guckenheimer and P. Holmes, *Global bifurcations. In nonlinear oscillations, dynamical systems, and bifurcations of vector fields*, Springer, New York, NY, 1983.

[29] C. Douskos and P. Markellos, "Complete coefficient criteria for five-dimensional Hopf bifurcations, with an application to economic dynamics," *Journal of Nonlinear Dynamics*, vol. 2015, Article ID 278234, 11 pages, 2015.

[30] J. Muller, *Mathematical models in biology*, Technical University Munich Centre for Mathematical Sciences, 2004.

[31] F. A. Ascioti, E. Beltrami, T. O. Carroll, and C. Wirick, "Is there chaos in plankton dynamics?," *Journal of Plankton Research*, vol. 15, no. 6, pp. 603–617, 1993.

[32] L. Stone and S. Ezrati, "Chaos, cycles and spatiotemporal dynamics in plant ecology," *Journal of Ecology*, vol. 84, no. 2, pp. 279–291, 1996.